

---

# OpenXAI: Towards a Transparent Evaluation of Post hoc Model Explanations

---

Chirag Agarwal<sup>1</sup>, Dan Ley<sup>1</sup>, Satyapriya Krishna<sup>1</sup>, Eshika Saxena<sup>\*1</sup>, Martin Pawelczyk<sup>1</sup>, Nari Johnson<sup>4</sup>, Isha Puri<sup>\*1</sup>, Marinka Zitnik<sup>1</sup>, and Himabindu Lakkaraju<sup>1</sup>

<sup>1</sup>Harvard University

<sup>4</sup>Carnegie Mellon University

## Abstract

While several types of post hoc explanation methods have been proposed in recent literature, there is very little work on systematically benchmarking these methods. Here, we introduce OpenXAI, a comprehensive and extensible open-source framework for evaluating and benchmarking post hoc explanation methods. OpenXAI comprises of the following key components: (i) a flexible synthetic data generator and a collection of diverse real-world datasets, pre-trained models, and state-of-the-art feature attribution methods, and (ii) open-source implementations of eleven quantitative metrics for evaluating faithfulness, stability (robustness), and fairness of explanation methods, in turn providing comparisons of several explanation methods across a wide variety of metrics, models, and datasets. OpenXAI is easily extensible, as users can readily evaluate custom explanation methods and incorporate them into our leaderboards. Overall, OpenXAI provides an automated end-to-end pipeline that not only simplifies and standardizes the evaluation of post hoc explanation methods, but also promotes transparency and reproducibility in benchmarking these methods. While the first release of OpenXAI supports only tabular datasets, the explanation methods and metrics that we consider are general enough to be applicable to other data modalities. OpenXAI datasets and models, implementations of state-of-the-art explanation methods and evaluation metrics, are publicly available at this [GitHub link](#).

## 1 Introduction

As predictive models are increasingly deployed in critical domains (e.g., healthcare, law, and finance), there has been a growing emphasis on explaining the predictions of these models to decision-makers (e.g., doctors, and judges) so that they can understand the rationale behind model predictions, and determine if and when to rely on these predictions. To this end, various techniques have been proposed in recent literature to generate post hoc explanations of individual predictions made by complex ML models. Several of such *local explanation methods* output the influence of each of the features on the model’s prediction, and are therefore referred to as *local feature attribution methods*. Due to their generality, feature attribution methods are increasingly being utilized to explain complex models in medicine, finance, law, and science [23, 34, 78]. Thus, it is critical to ensure that the explanations generated by these methods are *reliable* so that relevant stakeholders and decision makers are provided with credible information about the underlying models [6].

Prior works have studied several notions of explanation reliability such as *faithfulness* (or fidelity) [81, 51, 33], *stability* (or robustness) [7, 4], and *fairness* [18, 9], and proposed metrics for

---

<sup>\*</sup>Work done by authors when they were at Harvard University.

quantifying these notions. Many of these works also demonstrated through small-scale experiments or qualitative analysis that certain explanation methods are not effective w.r.t. specific notions of reliability. For instance, Alvarez-Melis and Jaakkola [7] visualized the explanations generated by some of the popular gradient based explanation methods [67, 66, 70, 72] for MNIST images, and showed that they are not robust to small input perturbations. However, it is unclear if such findings generalize beyond the settings studied. More broadly, one of the biggest open questions which has far-reaching implications for the progress of explainable AI (XAI) research is: *which explanation methods are effective w.r.t. which notions of reliability and under what conditions?* [43]. A first step towards answering this question involves systematically benchmarking explanation methods in a reproducible and transparent manner. However, the increasing diversity of explanation methods, and the plethora of evaluation settings and metrics outlined in existing research without standardized open-source implementations make it rather challenging to carry out such benchmarking efforts.

In this work, we address the aforementioned challenges by introducing OpenXAI, a comprehensive and extensible open-source framework for systematically and efficiently benchmarking explanation methods in a transparent and reproducible fashion. More specifically, our work makes the following key contributions:

1. We introduce the OpenXAI framework, an *open-source ecosystem* designed to support systematic, reproducible, and efficient evaluations of post hoc explanation methods. OpenXAI unifies the existing scattered repositories of datasets, models, and evaluation metrics, and provides a *simple and easy-to-use API* that enables researchers and practitioners to benchmark explanation methods using just a few lines of code (Section 2).
2. Our OpenXAI framework currently provides open-source implementations and ready-to-use API interfaces for *six state-of-the-art feature attribution methods* (LIME, SHAP, Vanilla Gradients, Gradient x Input, SmoothGrad, and Integrated Gradients), and *eleven quantitative metrics* to evaluate the faithfulness, stability, and fairness of feature attribution methods. In addition, it includes a comprehensive collection of *seven real-world datasets* spanning diverse real-world domains, and *sixteen different pre-trained models*. OpenXAI also introduces a *novel and flexible synthetic data generator* to synthesize datasets of varying sizes, complexity, and dimensionality which facilitate the construction of reliable ground truth explanations (Section 2).
3. The OpenXAI framework is *easily extensible* i.e., researchers and practitioners can readily incorporate custom explanation methods, datasets, predictive models, and evaluation metrics into our framework and benchmarks (Section 2).
4. Lastly, using OpenXAI, we *perform rigorous empirical benchmarking* of the aforementioned state-of-the-art feature attribution methods to determine which methods are effective w.r.t. what notions of reliability across a wide variety of datasets and predictive models (Section 3).

Overall, our OpenXAI framework provides an end-to-end pipeline that unifies, simplifies, and standardizes several existing workflows to evaluate explanation methods. By enabling systematic and efficient evaluation and benchmarking of existing and new explanation methods, our OpenXAI framework can inform and accelerate new research in the emerging field of XAI. OpenXAI will be regularly updated and welcomes input from the community.

**Related Work.** Our work builds on the vast literature in explainable AI. Here, we discuss closely related works and their connections to our benchmark (see the Appendix for further discussion).

*Evaluation Metrics for Post hoc Explanations:* Prior research has studied several notions of explanation reliability, namely, *faithfulness* (or fidelity), *stability* (or robustness), and *fairness* [51, 81, 7, 18]. While the faithfulness notion captures how faithfully a given explanation captures the true behavior of the underlying model [81, 51, 33], stability ensures that explanations do not change drastically with small perturbations to the input [29, 7]. The fairness notion, on the other hand, ensures that there are no group-based disparities in the faithfulness or stability of explanations [18]. To this end, prior works [51, 69, 81, 7, 18, 33] proposed various evaluation metrics to quantify the aforementioned notions. For instance, Petsiuk et al. [59] measured the change in the probability of the predicted class when important features (as identified by an explanation) are deleted from or introduced into the data instance. A sharp change in the probability implies a high degree of explanation faithfulness. Alvarez-Melis and Jaakkola [7] loosely quantified stability as the maximum change in the resulting explanations when small perturbations are made to a given instance. Dai et al.

[18] quantified unfairness of explanations as the difference between the faithfulness (or stability) metric values averaged over instances in the majority and the minority subgroups.

*XAI Libraries and Benchmarks:* Prior works have introduced XAI libraries and benchmarks, the most popular among them being Captum [42], Quantus [32], XAI-Bench [51], and SHAP Benchmark. Below, we provide a brief description for each, and detail how our work differs from them.

While *Captum library* [42] is an open-source library that provides implementations and APIs for various state-of-the-art explanation methods, its focus is not on evaluating and/or benchmarking these methods which is the main goal of our work. *Quantus library* [32], on the other hand, provides implementations of certain evaluation metrics to measure the faithfulness and stability/robustness of explanation methods. However, it does not focus on benchmarking explanation methods or providing public dashboards to compare the performance of these methods. Furthermore, the stability/robustness measures [7] supported by Quantus are somewhat outdated and have been superseded by recently proposed metrics [4]. In addition, Quantus does not support any fairness metrics to evaluate disparities in the quality of explanations which is very important in real-world settings such as healthcare, criminal justice, and policy. In contrast, OpenXAI not only subsumes popular faithfulness and stability/robustness metrics supported by Quantus but also supports 7 new metrics to measure the faithfulness, stability/robustness, as well as the fairness of explanation methods [4, 18, 43]. In addition, OpenXAI focuses on systematically benchmarking state-of-the-art explanation methods and providing public dashboards to readily compare these methods.

*SHAP benchmark* [2] only focuses on evaluating and comparing different variants of SHAP [54] via certain faithfulness metrics which are similar to the Prediction Gap on Important (PGI) and Unimportant (PGU) feature perturbation metrics outlined in our work. Note that the SHAP benchmark does not include any stability/robustness or fairness metrics. In contrast, OpenXAI benchmarks these metrics extensively across a variety of explanation methods (e.g., LIME, Gradient-based methods).

*XAI-Bench* [51] constructed synthetic datasets with ground truth explanations to evaluate the faithfulness of a few explanation methods (e.g., LIME, SHAP, MAPLE). However, recent research argued that their evaluation is unreliable, and predictive models learned using their synthetic datasets may not adhere to the ground truth explanations [24]. In addition, the aforementioned evaluation is rather limited in scope as synthetic datasets may not even be representative of real-world data [24]. In contrast, our work not only proposes a novel synthetic data generator that addresses the shortcomings of the synthetic datasets constructed in XAI-Bench but also facilitates the evaluation and benchmarking of the faithfulness, stability, as well as the fairness of 6 state-of-the-art explanation methods on 7 real-world datasets with no ground truth explanations.

In summary, our work makes the following key contributions:

- We provide implementations and easy-to-use API interfaces for 11 metrics to evaluate the faithfulness, stability, and fairness of explanation methods, 7 of which have not been implemented in prior libraries or benchmarks – the faithfulness metrics Feature Agreement (FA), Rank Agreement (RA), Sign Agreement (SA), Signed Rank Agreement (SRA), Pairwise Rank Agreement (PRA), and the stability metrics Relative Representation Stability (RRS) and Relative Output Stability (ROS).
- We also introduce a novel and flexible synthetic data generator to synthesize datasets of varying sizes, complexity, and dimensionality to facilitate the construction of reliable ground truth explanations in order to evaluate state-of-the-art explanation methods. Our synthetic data generator addresses the shortcomings of the prior synthetic benchmark (XAI-Bench) by generating synthetic datasets which encapsulate certain key properties, namely, unambiguously defined local neighborhoods, a clear description of feature importances in each local neighborhood, and feature independence. These properties, in turn, allow us to theoretically guarantee that any accurate model trained on our synthetic datasets will adhere to the ground truth explanations of the underlying data.
- We perform rigorous empirical benchmarking of 6 state-of-the-art feature attribution methods using our OpenXAI framework to determine which methods are effective w.r.t. each of the 11 evaluation metrics across 8 real-world/synthetic datasets, and 16 different predictive models. Note that none of the previously proposed libraries or benchmarks carry out such exhaustive benchmarking efforts across such a wide variety of metrics, models, and datasets.

## 2 Overview of OpenXAI Framework

OpenXAI provides a comprehensive programmatic environment with synthetic and real-world datasets, data processing functions, explainers, and evaluation metrics to rigorously and efficiently benchmark explanation methods. Below, we discuss each of these components in detail.

**1) Datasets and Predictive Models.** The current release of our OpenXAI framework includes a collection of eight different synthetic and real-world datasets. While synthetic datasets allow us to construct ground truth explanations which can then be used to evaluate explanations output by state-of-the-art methods, real-world datasets (where it is typically hard to construct ground truth explanations) help us benchmark these methods in a more realistic manner suitable for practical applications [51]. We would like to note that OpenXAI includes datasets that are widely employed in XAI research to evaluate the efficacy of newly proposed methods and study the behavior of existing methods [9, 18–20, 38, 69, 73].

*Synthetic Datasets:* While prior research [51, 41] proposed methods to generate synthetic datasets and corresponding ground truth explanations, they all suffer from a significant drawback as demonstrated by Faber et al. [24] – there is no guarantee that the models trained on these datasets will adhere to the ground truth explanations of the underlying data. This, in turn, implies that evaluating post hoc explanations using the above ground truth explanations would be incorrect since post hoc explanations are supposed to reliably explain the behavior of the underlying model, and not that of the underlying data. To illustrate, let us consider the case where we use aforementioned methods to construct a synthetic dataset with features  $A, B, C$ , and  $D$  such that the ground truth labels only depend on features  $A$  and  $B$  i.e., the ground truth explanation of the underlying data indicates that features  $A$  and  $B$  are most important. If we train a model on this data and if features  $A$  and  $B$  are correlated with  $C$  and  $D$  respectively, then the resulting model may base its predictions on  $C$  and  $D$  (and not  $A$  and  $B$ ) and still be very accurate. If a post hoc explanation of this model then (correctly) indicates that the most important features of the model are  $C$  and  $D$ , this explanation may be deemed incorrect if we compare it against the ground truth explanation of the underlying data. This problem further exacerbates as we increase the complexity of the ground truth labeling function [24].

To address the aforementioned challenges, we develop a novel synthetic data generation mechanism, *SynthGauss*, which encapsulates three key properties, namely, feature independence, unambiguously-defined local neighborhoods, and a clear description of feature influence in each local neighborhood. Intuitively, this approach generates  $K$  well-separated clusters where points in each cluster  $k \in \{1, 2, \dots, K\}$  are sampled from a Gaussian distribution  $\mathcal{N}(\mu_k, \Sigma_k)$  where  $\mu_k \in \mathbb{R}^d$  is the mean and  $\Sigma_k \in \mathbb{R}^{d \times d}$  is the covariance matrix. While this parameterization is general enough to support the construction of synthetic datasets of  $K$  clusters with varying means and covariances, we set the means of all the clusters such that the intracluster distances are significantly smaller than the intercluster distances, and we set the covariance matrices of all the clusters to identity. This ensures that all the features are independent, and local neighborhoods (clusters) are unambiguously defined.

We then generate ground truth labels for instances by first randomly sampling feature mask vectors  $m_k \in \{0, 1\}^d$  (vectors comprising of 0s and 1s) for each cluster  $k$ . The vector  $m_k$  determines which features influence the ground truth labeling process for instances in cluster  $k$  (a value of 1 indicates that the corresponding feature is influential). We then randomly sample feature weight vectors  $w_k \in \mathbb{R}^d$  which capture the relative importance of each of the features in the labeling process of instances in each cluster  $k$ . The ground truth labels of instances in each cluster  $k$  are then computed as a function (e.g., sigmoid) of the feature values of individual instances, and the dot product of the corresponding cluster’s feature mask vector and weight vector i.e.,  $m_k \odot w_k$ . Complete pseudocode and other details of this generation process are included in the Appendix. Note that  $m_k$  corresponds to the ground truth explanation for all instances in cluster  $k$ . Since our generation process is designed to encapsulate feature independence, unambiguous definitions of local neighborhoods, and clear descriptions of feature influences, any accurate model trained on the resulting dataset will adhere to the ground truth explanations of the underlying data (See Theorem 1 in Appendix).

*Real-world Datasets:* In the current release of OpenXAI, we include seven real-world datasets that are highly diverse in terms of several key properties. They comprise of data spanning multiple real-world domains (e.g., finance, lending, healthcare, and criminal justice), varying dataset sizes (e.g., small vs. large-scale), dimensionalities (e.g., low vs. high dimensional), class imbalance ratios, and feature types (e.g., continuous vs. discrete). We focus on tabular data in this release as such

data is commonly encountered in real-world applications where explainability is critical [75], and has also been widely studied in XAI literature [51]. Table 1 provides a summary of the real-world datasets currently included in OpenXAI. See Section D.1 in the Appendix for detailed descriptions of individual datasets. While these real-world datasets are primarily drawn from prior research and existing repositories, OpenXAI provides comprehensive data loading and pre-processing capabilities to make these datasets *XAI-ready* (further details below).

**Table 1: Summary of currently available datasets in OpenXAI.** Here, “Feature Types” denotes whether features in the dataset are discrete or continuous, “Feature Information” describes what kind of information is captured in the dataset, and “Balanced” denotes whether the dataset is balanced w.r.t. the predictive label.

Dataset	Size	# Features	Feature Types	Feature Information	Balanced
Synthetic Data	5,000	20	continuous	synthetic	✓
German Credit [22]	1,000	20*	discrete, continuous	demographic, personal, financial	✗
HELOC [25]	9,871	23	continuous	demographic, financial	✓
Adult Income [79]	45,222	13	discrete, continuous	demographic, personal, education/employment, financial	✗
COMPAS [36]	6,172	7	discrete, continuous	demographic, personal, criminal	✗
Give Me Some Credit [27]	102,209	10	discrete, continuous	demographic, personal, financial	✗
Pima-Indians	768	8	discrete, continuous	demographic, healthcare	✗
Diabetes [71]					
Framingham Heart Study [1]	3,658	15	continuous	demographic, healthcare	✗

\*expands to 60 features after one hot encoding of discrete features

**Dataloaders:** OpenXAI provides a `ReturnLoaders` function that can be used to load the aforementioned collection of synthetic and real-world datasets as well as any other custom datasets, and ensures that they are *XAI-ready*. More specifically, this class takes as input the name of an existing OpenXAI dataset and outputs a train set which can then be used to train a predictive model, and a test set which can be used to generate local explanations of the trained model. The code snippet below shows how to import the `ReturnLoaders` function and load an existing OpenXAI dataset.

```
from openxai.dataloader import ReturnLoaders
trainloader, testloader = ReturnLoaders(data_name='german', download=True)
inputs, labels = next(iter(testloader))
```

**Pre-trained models:** We train two classes of predictive models (artificial neural networks and logistic regression models) and incorporate them into the OpenXAI framework so that they can be readily used for benchmarking explanation methods. The code snippet below shows how to load OpenXAI’s pre-trained models using our `LoadModel` function.

```
from openxai.model import LoadModel
model = LoadModel(data_name='german', ml_model='ann')
```

**2) Explainers.** OpenXAI provides ready-to-use implementations of six state-of-the-art feature attribution methods, namely, LIME, SHAP, Vanilla Gradients, Gradient x Input, SmoothGrad, and Integrated Gradients. An implementation of a random baseline which randomly assigns importance values to each of the features, and returns these random assignments as explanations is also included. Our implementations of these methods build on other open-source libraries (e.g., Captum [42]) as well as their original implementations. While methods such as LIME and SHAP leverage perturbations of data instances and their corresponding model predictions to *learn* a local explanation model, they do not require access to the internals of the models or their gradients. On the other hand, Vanilla Gradients, Gradient x Input, SmoothGrad, and Integrated Gradients require access to the gradients of the underlying models but do not need to repeatedly query the models for their predictions (see Table 6 in Appendix for a brief summary of these methods). These differences influence the efficiency with which explanations can be generated by these methods. OpenXAI provides an abstract `Explainer` class which enables us to load existing explanation methods as well as integrate new explanation methods.

```

from openxai.explainer import Explainer
exp_method = Explainer(method='shap', model=model)
explanations = exp_method.get_explanations(inputs)

```

All the explanation methods included in OpenXAI are readily accessible through the Explainer class, and users just have to specify the method name in order to invoke the appropriate method and generate explanations as shown in the above code snippet. Users can easily incorporate their own custom explanation methods into the OpenXAI framework by extending the Explainer class and including the code for their methods in the get\_explanations function (see template above) of this class. They can then submit a request to incorporate their custom methods into OpenXAI.

**3) Evaluation Metrics.** OpenXAI provides implementations and ready-to-use APIs for a set of twenty-two quantitative metrics proposed by prior research to evaluate the faithfulness, stability, and fairness of explanation methods. OpenXAI is the first XAI benchmark to consider all the three aforementioned aspects of explanation reliability. More specifically, we include eight different metrics to measure explanation faithfulness (both with and without ground truth explanations) [43, 59], and three different metrics to measure stability [4]. Below, we briefly describe these metrics. Detailed descriptions of all the metrics along with notation and equations are included in the Appendix.

a) *Ground-truth Faithfulness:* Krishna et al. [43] recently proposed six evaluation metrics to capture the similarity between the top-K or a select set of features of any two feature attribution-based explanations. We leverage these metrics to capture the similarity between the explanations output by state-of-the-art methods and the ground-truth explanations constructed using our synthetic data generation process. These metrics and their definitions are given as follows: i) Feature Agreement (FA) which computes the fraction of top-K features that are common between a given post hoc explanation and the corresponding ground truth explanation, ii) Rank Agreement (RA) metric which measures the fraction of top-K features that are not only common between a given post hoc explanation and the corresponding ground truth explanation, but also have the same position in the respective rank orders, iii) Sign Agreement (SA) metric which computes the fraction of top-K features that are not only common between a given post hoc explanation and the corresponding ground truth explanation, but also share the same sign (direction of contribution) in both the explanations, iv) Signed Rank Agreement (SRA) metric which computes the fraction of top-K features that are not only common between a given post hoc explanation and the corresponding ground truth explanation, but also share the same feature attribution sign (direction of contribution) and position (rank) in both the explanations, v) Rank Correlation (RC) metric which computes Spearman’s rank correlation coefficient to measure the agreement between feature rankings provided by a given post hoc explanation and the corresponding ground truth explanation, and vi) Pairwise Rank Agreement (PRA) metric which captures if the relative ordering of every pair of features is the same for a given post hoc explanation as well as the corresponding ground-truth explanation.

b) *Predictive Faithfulness:* We leverage the metrics outlined by [59, 18] to measure the faithfulness of an explanation when no ground truth is available. This metric, referred to as Prediction Gap on Important feature perturbation (PGI), computes the difference in prediction probability that results from perturbing the features deemed as influential by a given post hoc explanation. Higher values on this metric imply greater explanation faithfulness. We also consider the converse of this metric, Prediction Gap on Unimportant feature perturbation (PGU), which perturbs the unimportant features and measures the change in prediction probability.

c) *Stability:* We consider the metrics introduced by Alvarez-Melis and Jaakkola [7], Agarwal et al. [4] to measure how robust a given explanation is to small input perturbations. More specifically, we leverage the metrics Relative Input Stability (RIS), Relative Representation Stability (RRS), and Relative Output Stability (ROS) which measure the maximum change in explanation relative to changes in the inputs, model parameters, and output prediction probabilities respectively.

d) *Fairness:* Following the work by Dai et al. [18], we measure the fairness of post hoc explanations by averaging all the aforementioned metric values across instances in the majority and minority subgroups, and comparing the two estimates. If there is a huge difference in the two estimates, then we consider this to be evidence for unfairness.

Invoking the aforementioned metrics to benchmark an explanation methods is quite simple and the code snippet below describes how to invoke the PGI metric (where kwargs represents a dictionary containing the given metric’s parameters).

```

from openxai.evaluator import Evaluator
metric_evaluator = Evaluator(model, metric='PGI')
score, mean_score = metric_evaluator.evaluate(**kwargs)

```

**Benchmarking:** As can be seen from the code snippets in this section, OpenXAI allows end users to easily benchmark explanation methods using just a few lines of code. To summarize the benchmarking process, let us consider a scenario where we would like to benchmark a new explanation method using OpenXAI’s pre-trained neural network model and the German Credit dataset. First, we use OpenXAI’s `ReturnLoaders` function to load the German Credit dataset. Second, we load the neural network model (‘ann’) using our `LoadModel` function. Third, we extend the `Explainer` class and incorporate the code for the new explanation method in the `get_explanations` function of this class. Finally, we evaluate the new explanation method using any metric from the `Evaluator` class.

### 3 Benchmarking Analysis

Next, we describe how we benchmark state-of-the-art explanation methods using our OpenXAI framework and also discuss the key findings of this benchmarking analysis. Code to reproduce all the results is available at <https://github.com/AI4LIFE-GROUP/OpenXAI>.

**Experimental Setup.** We benchmark all of the six state-of-the-art feature attribution methods currently available in our OpenXAI framework along with the random baseline, using the `openxai.Evaluator` module (See Section 2), and for the first 1000 test instances of each dataset. Details about the hyperparameters used in our experiments are discussed in Section D.3 in the Appendix. Our OpenXAI framework currently has two pre-trained models, a logistic regression model and a deep neural network model, for each dataset. The neural network models have two fully connected hidden layers with 100 nodes in each layer, and they use ReLU activation functions and an output softmax layer. See Appendix D.4 for details on model architectures, training and performance.

**Faithfulness.** We evaluate the ground-truth and predictive faithfulness of explanations generated by state-of-the-art methods using both synthetic and real-world datasets.

*Ground-truth faithfulness:* For logistic regression models, we evaluate ground-truth faithfulness by calculating the similarity between the generated explanations and the ground-truth explanations using the metrics discussed in Section 2. Results for various ground-truth faithfulness metrics are shown in Tables 2-3, 8-9, 16-19. Vanilla Gradients, Integrated Gradients, and SmoothGrad produce explanations that achieve perfect scores on four ground-truth faithfulness metrics, viz. pairwise rank agreement (PRA), rank correlation (RC), feature agreement (FA), rank agreement (RA), sign agreement (SA), signed rank agreement (SRA) metrics, for all datasets. LIME outperforms other methods, approaching the performance of the above gradient-based explanations in many cases. While illustrative in nature, these findings show how OpenXAI can help identify the limitations of existing explanation methods, which in turn can inform the design of new methods.

*Predictive faithfulness:* Tables 2-3, 8-9, 16-19 show results for logistic regression models, and Tables 10-11, 24-29 show results for neural network models on the PGI and PGU metrics implemented in OpenXAI (see Section 2 and Appendix A). Overall, we find that Vanilla Gradients, SmoothGrad, and LIME explanations are most faithful to the underlying model and, on average across all datasets and models, outperform other feature-attribution methods on the PGI metric. The PGU metric showed similar trends in terms of best performance, with Integrated Gradients on par with the leading metrics.

**Stability.** Next, we examine the stability of explanation methods when the underlying models are logistic regression models in Tables 4-5 below (additionally, Tables 12-13, 20- 23 in the Appendix), and neural network models (Tables 14-15, 30- 35). For logistic regression models, we consider only the RIS and ROS metrics for stability, since RRS is equivalent to ROS within this model class. Overall, we see similar trends across explanation methods for each of the relative stability metrics at our chosen set of hyperparameters (see Appendix D.3). First, Integrated Gradients tends to outperform all other feature-attribution methods with log average scores of 1.95 and 1.86 for RIS and ROS, respectively, when averaged across all datasets. Vanilla Gradients and Gradient x Input remain on roughly the same order of magnitude with log average scores of 3.16 and 3.37 for RIS, and 2.91 and 4.49 for ROS. The remaining methods, LIME, SHAP, SmoothGrad and Random, score log RIS and ROS scores between roughly 10 and 15.

**Table 2: Ground-truth and predictive faithfulness results on the HELOC dataset for all explanation methods with LR model.** Shown are average and standard error metric values computed across 1000 test instances.  $\uparrow$  indicates that higher values are better, and  $\downarrow$  indicates that lower values are better. Values corresponding to best performance are bolded.

Method	PRA ( $\uparrow$ )	RC ( $\uparrow$ )	FA ( $\uparrow$ )	RA ( $\uparrow$ )	SA ( $\uparrow$ )	SRA ( $\uparrow$ )	PGU ( $\downarrow$ )	PGI ( $\uparrow$ )
Random	0.500 $\pm$ 0.00	0.002 $\pm$ 0.01	0.149 $\pm$ 0.00	0.046 $\pm$ 0.00	0.076 $\pm$ 0.00	0.024 $\pm$ 0.00	0.098 $\pm$ 0.00	0.039 $\pm$ 0.00
VanillaGrad	<b>1.000</b> $\pm$ 0.00	<b>1.000</b> $\pm$ 0.00	<b>1.000</b> $\pm$ 0.00	<b>1.000</b> $\pm$ 0.00	<b>1.000</b> $\pm$ 0.00	<b>1.000</b> $\pm$ 0.00	<b>0.073</b> $\pm$ 0.00	<b>0.076</b> $\pm$ 0.00
IntegratedGrad	<b>1.000</b> $\pm$ 0.00	<b>1.000</b> $\pm$ 0.00	<b>1.000</b> $\pm$ 0.00	<b>1.000</b> $\pm$ 0.00	<b>1.000</b> $\pm$ 0.00	<b>1.000</b> $\pm$ 0.00	<b>0.073</b> $\pm$ 0.00	<b>0.076</b> $\pm$ 0.00
Gradient x Input	0.599 $\pm$ 0.00	0.291 $\pm$ 0.01	0.205 $\pm$ 0.00	0.029 $\pm$ 0.00	0.205 $\pm$ 0.00	0.029 $\pm$ 0.00	0.096 $\pm$ 0.00	0.046 $\pm$ 0.00
SmoothGrad	<b>1.000</b> $\pm$ 0.00	<b>1.000</b> $\pm$ 0.00	<b>1.000</b> $\pm$ 0.00	<b>1.000</b> $\pm$ 0.00	<b>1.000</b> $\pm$ 0.00	<b>1.000</b> $\pm$ 0.00	<b>0.073</b> $\pm$ 0.00	<b>0.076</b> $\pm$ 0.00
SHAP	0.603 $\pm$ 0.00	0.291 $\pm$ 0.01	0.195 $\pm$ 0.00	0.029 $\pm$ 0.00	0.195 $\pm$ 0.00	0.029 $\pm$ 0.00	0.096 $\pm$ 0.00	0.045 $\pm$ 0.00
LIME	0.923 $\pm$ 0.00	0.946 $\pm$ 0.00	0.910 $\pm$ 0.00	0.682 $\pm$ 0.01	0.910 $\pm$ 0.00	0.682 $\pm$ 0.01	<b>0.073</b> $\pm$ 0.00	<b>0.076</b> $\pm$ 0.00

**Table 3: Ground-truth and predictive faithfulness results on the Adult Income dataset for all explanation methods with LR model.** Shown are average and standard error metric values computed across 1000 test instances.  $\uparrow$  indicates that higher values are better, and  $\downarrow$  indicates that lower values are better. Values corresponding to best performance are bolded.

Method	PRA ( $\uparrow$ )	RC ( $\uparrow$ )	FA ( $\uparrow$ )	RA ( $\uparrow$ )	SA ( $\uparrow$ )	SRA ( $\uparrow$ )	PGU ( $\downarrow$ )	PGI ( $\uparrow$ )
Random	0.501 $\pm$ 0.00	0.003 $\pm$ 0.01	0.188 $\pm$ 0.01	0.073 $\pm$ 0.00	0.093 $\pm$ 0.00	0.034 $\pm$ 0.00	0.130 $\pm$ 0.00	0.043 $\pm$ 0.00
VanillaGrad	<b>1.000</b> $\pm$ 0.00	<b>1.000</b> $\pm$ 0.00	0.999 $\pm$ 0.00	0.998 $\pm$ 0.00	0.999 $\pm$ 0.00	0.998 $\pm$ 0.00	0.065 $\pm$ 0.00	0.124 $\pm$ 0.00
IntegratedGrad	<b>1.000</b> $\pm$ 0.00	<b>1.000</b> $\pm$ 0.00	<b>1.000</b> $\pm$ 0.00	<b>1.000</b> $\pm$ 0.00	<b>1.000</b> $\pm$ 0.00	<b>1.000</b> $\pm$ 0.00	0.065 $\pm$ 0.00	0.124 $\pm$ 0.00
Gradient x Input	0.538 $\pm$ 0.00	0.215 $\pm$ 0.00	0.359 $\pm$ 0.00	0.138 $\pm$ 0.01	0.359 $\pm$ 0.00	0.138 $\pm$ 0.01	0.124 $\pm$ 0.00	0.062 $\pm$ 0.00
SmoothGrad	<b>1.000</b> $\pm$ 0.00	<b>1.000</b> $\pm$ 0.00	0.999 $\pm$ 0.00	0.999 $\pm$ 0.00	0.999 $\pm$ 0.00	0.999 $\pm$ 0.00	0.065 $\pm$ 0.00	0.124 $\pm$ 0.00
SHAP	0.627 $\pm$ 0.00	0.319 $\pm$ 0.01	0.363 $\pm$ 0.00	0.041 $\pm$ 0.00	0.362 $\pm$ 0.00	0.041 $\pm$ 0.00	0.125 $\pm$ 0.00	0.062 $\pm$ 0.00
LIME	0.881 $\pm$ 0.00	0.876 $\pm$ 0.00	0.924 $\pm$ 0.00	0.875 $\pm$ 0.00	0.924 $\pm$ 0.00	0.875 $\pm$ 0.00	<b>0.063</b> $\pm$ 0.00	<b>0.126</b> $\pm$ 0.00

**Table 4: Stability results on the Synthetic dataset for all explanation methods with LR model.** Shown are log average and standard error metric values computed across 1000 test instances.  $\uparrow$  indicates that higher values are better, and  $\downarrow$  indicates that lower values are better. Values corresponding to best performance are bolded.

Method	RIS ( $\downarrow$ )	ROS ( $\downarrow$ )
Random	11.58 $\pm$ 0.00	12.34 $\pm$ 0.02
VanillaGrad	2.49 $\pm$ 0.01	0.85 $\pm$ 0.04
IntegratedGrad	<b>1.17</b> $\pm$ 0.01	<b>-0.70</b> $\pm$ 0.02
Gradient x Input	2.50 $\pm$ 0.01	2.82 $\pm$ 0.04
SmoothGrad	9.69 $\pm$ 0.01	11.25 $\pm$ 0.02
SHAP	9.35 $\pm$ 0.01	11.69 $\pm$ 0.02
LIME	9.10 $\pm$ 0.02	12.17 $\pm$ 0.04

**Table 5: Stability results on the German Credit dataset for all explanation methods with LR model.** Shown are log average and standard error metric values computed across 1000 test instances.  $\uparrow$  indicates that higher values are better, and  $\downarrow$  indicates that lower values are better. Values corresponding to best performance are bolded.

Method	RIS ( $\downarrow$ )	ROS ( $\downarrow$ )
Random	12.84 $\pm$ 0.00	14.78 $\pm$ 0.04
VanillaGrad	-0.01 $\pm$ 0.04	-0.21 $\pm$ 0.07
IntegratedGrad	<b>-0.78</b> $\pm$ 0.03	<b>-1.20</b> $\pm$ 0.05
Gradient x Input	0.47 $\pm$ 0.01	3.10 $\pm$ 0.09
SmoothGrad	8.87 $\pm$ 0.03	10.71 $\pm$ 0.07
SHAP	10.01 $\pm$ 0.07	13.88 $\pm$ 0.10
LIME	9.59 $\pm$ 0.01	11.34 $\pm$ 0.05

**Fairness.** To measure fairness of explanation methods, we compute the average metric values (for each of the aforementioned faithfulness and stability metrics) for different subgroups (e.g., male and female) in the dataset and compare them. Larger gaps between the metric values for different subgroups indicates higher disparities (unfairness). We present results for the PGU (see Section 2 and Appendix A) metric. The fairness analysis in Figures 1 and 2 shows that there are disparities in the faithfulness of explanations (see Section 2) output by several methods (most notably, Gradient x Input and SHAP on the Adult Income dataset). Results with NN models are included in Appendix D.7.



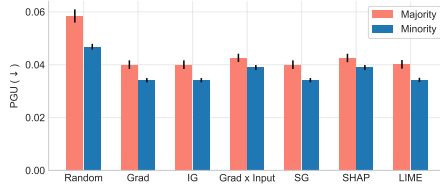


**Figure 1: Fairness analysis of PGU metric on the German Credit dataset with LR model.** Shown are average and standard error values for majority (male) and minority (female) subgroups. Larger gaps between the values of majority and minority subgroups (*i.e.*, red and blue bars respectively) indicate higher disparities which are undesirable.

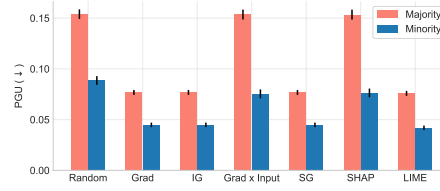


**Figure 2: Fairness analysis of PGU metric on the Adult Income dataset with LR model.** Shown are average and standard error values for the majority (male) and minority (female) subgroups. Larger gaps between the values of majority and minority subgroups (*i.e.*, red and blue bars respectively) indicate higher disparities which are undesirable.

## 4 Conclusion

As post hoc explanations are increasingly being employed to aid decision makers and relevant stakeholders in various high-stakes applications, it becomes important to ensure that these explanations are reliable. To this end, we introduce OpenXAI, an open-source ecosystem comprising of XAI-ready datasets, implementations of state-of-the-art explanation methods, evaluation metrics, leaderboards and documentation to promote transparency and collaboration around evaluations of post hoc explanations. OpenXAI can readily be used to benchmark new explanation methods as well as incorporate them into our framework and leaderboards. By enabling systematic and efficient evaluation and benchmarking of existing and new explanation methods, OpenXAI can inform and accelerate new research in the emerging field of XAI. OpenXAI will be regularly updated with new datasets, explanation methods, and evaluation metrics, and welcomes input from the community.

## Acknowledgments and Disclosure of Funding

The authors would like to thank the anonymous reviewers for their helpful feedback and all the funding agencies listed below for supporting this work. This work is supported in part by the NSF awards #IIS-2008461 and #IIS-2040989, and research awards from Google, JP Morgan, Amazon, Harvard Data Science Initiative, and D<sup>3</sup> Institute at Harvard. HL would like to thank Sujatha and Mohan Lakkaraju for their continued support and encouragement. The views expressed here are those of the authors and do not reflect the official policy or position of the funding agencies.

## References

- [1] Framingham heart study dataset | kaggle. <https://www.kaggle.com/datasets/aasheesh200/framingham-heart-study-dataset>. (Accessed on 08/15/2022).
- [2] Shap benchmark. URL <https://shap.readthedocs.io/en/latest/index.html>.
- [3] Chirag Agarwal and Anh Nguyen. Explaining image classifiers by removing input features using generative models. In *ACCV*, 2020.
- [4] Chirag Agarwal, Nari Johnson, Martin Pawelczyk, Satyapriya Krishna, Eshika Saxena, Marinka Zitnik, and Himabindu Lakkaraju. Rethinking stability for attribution-based explanations. In *ICLR 2022 Workshop on PAIR<sup>2</sup> Struct*, 2022.
- [5] Sushant Agarwal, Shahin Jabbari, Chirag Agarwal, Sohini Upadhyay, Steven Wu, and Himabindu Lakkaraju. Towards the unification and robustness of perturbation and gradient based explanations. In *ICML*, 2021.
- [6] Ulrich Aivodji, Hiromi Arai, Olivier Fortineau, Sébastien Gambs, Satoshi Hara, and Alain Tapp. Fairwashing: the risk of rationalization. In *ICML*, 2019.
- [7] David Alvarez-Melis and Tommi S Jaakkola. On the robustness of interpretability methods. *arXiv*, 2018.

- [8] Alejandro Barredo Arrieta, Natalia Díaz-Rodríguez, Javier Del Ser, Adrien Bennetot, Siham Tabik, Alberto Barbado, Salvador García, Sergio Gil-López, Daniel Molina, Richard Benjamins, et al. Explainable artificial intelligence (xai): Concepts, taxonomies, opportunities and challenges toward responsible ai. *Information Fusion*, 2020.
- [9] Aparna Balagopalan, Haoran Zhang, Kimia Hamidieh, Thomas Hartvigsen, Frank Rudzicz, and Marzyeh Ghassemi. The road to explainability is paved with bias: Measuring the fairness of explanations. *arXiv*, 2022.
- [10] Naman Bansal, Chirag Agarwal, and Anh Nguyen. Sam: The sensitivity of attribution methods to hyperparameters. In *CVPR*, 2020.
- [11] Solon Barocas, Andrew Selbst, and Manish Raghavan. The hidden assumptions behind counterfactual explanations and principal reasons. In *FAccT*, 2020.
- [12] Osbert Bastani, Carolyn Kim, and Hamsa Bastani. Interpretability via model extraction. *arXiv*, 2017.
- [13] Jacob Bien and Robert Tibshirani. Classification by set cover: The prototype vector machine. *arXiv*, 2009.
- [14] Vadim Borisov, Tobias Leemann, Kathrin Seßler, Johannes Haug, Martin Pawelczyk, and Gjergji Kasneci. Deep neural networks and tabular data: A survey. *arXiv*, 2021.
- [15] Rich Caruana, Yin Lou, Johannes Gehrke, Paul Koch, Marc Sturm, and Noemie Elhadad. Intelligible models for healthcare: Predicting pneumonia risk and hospital 30-day readmission. In *KDD*, 2015.
- [16] Valerie Chen, Nari Johnson, Nicholay Topin, Gregory Plumb, and Ameet Talwalkar. Use-case-grounded simulations for explanation evaluation. *arXiv*, 2022.
- [17] Ian Covert, Scott Lundberg, and Su-In Lee. Explaining by removing: A unified framework for model explanation. *JMLR*, 2021.
- [18] Jessica Dai, Sohini Upadhyay, Ulrich Aivodji, Stephen H Bach, and Himabindu Lakkaraju. Fairness via explanation quality: Evaluating disparities in the quality of post hoc explanations. In *AAAI Conference on AI, Ethics, and Society (AIES)*, 2022.
- [19] Sanjoy Dasgupta, Nave Frost, and Michal Moshkovitz. Framework for evaluating faithfulness of local explanations. *arXiv*, 2022.
- [20] Ricardo Dominguez-Olmedo, Amir H Karimi, and Bernhard Schölkopf. On the adversarial robustness of causal algorithmic recourse. In *ICML*. PMLR, 2022.
- [21] Finale Doshi-Velez and Been Kim. Towards a rigorous science of interpretable machine learning. *arXiv*, 2017.
- [22] Dheeru Dua and Casey Graff. UCI machine learning repository, 2017. URL <http://archive.ics.uci.edu/ml>.
- [23] Radwa Elshawi, Mouaz H Al-Mallah, and Sherif Sakr. On the interpretability of machine learning-based model for predicting hypertension. *BMC medical informatics and decision making*, 2019.
- [24] Lukas Faber, Amin K. Moghaddam, and Roger Wattenhofer. When comparing to ground truth is wrong: On evaluating gnn explanation methods. In *KDD*, 2021.
- [25] FICO. Explainable machine learning challenge. <https://community.fico.com/s/explainable-machine-learning-challenge?tabset-158d9=3>, 2022. (Accessed on 05/23/2022).
- [26] Hidde Fokkema, Rianne de Heide, and Tim van Erven. Attribution-based explanations that provide recourse cannot be robust. *arXiv*, 2022.

- [27] Bryce Freshcorn. Give me some credit :: 2011 competition data | kaggle. <https://www.kaggle.com/datasets/brycecf/give-me-some-credit-dataset>, 2022. (Accessed on 05/23/2022).
- [28] Marzyeh Ghassemi, Luke Oakden-Rayner, and Andrew L Beam. The false hope of current approaches to explainable artificial intelligence in health care. *The Lancet Digital Health*, 2021.
- [29] Amirata Ghorbani, Abubakar Abid, and James Zou. Interpretation of neural networks is fragile. In *AAAI Conference on Artificial Intelligence*, 2019.
- [30] Riccardo Guidotti, Anna Monreale, Salvatore Ruggieri, Franco Turini, Fosca Giannotti, and Dino Pedreschi. A survey of methods for explaining black box models. *ACM computing surveys (CSUR)*, 2018.
- [31] Tessa Han, Suraj Srinivas, and Himabindu Lakkaraju. Which explanation should i choose? a function approximation perspective to characterizing post hoc explanations. *arXiv*, 2022.
- [32] Anna Hedström, Leander Weber, Dilyara Bareeva, Franz Motzkus, Wojciech Samek, Sebastian Lapuschkin, and Marina M-C Höhne. Quantus: an explainable ai toolkit for responsible evaluation of neural network explanations. *arXiv*, 2022.
- [33] Sara Hooker, Dumitru Erhan, Pieter-Jan Kindermans, and Been Kim. Evaluating feature importance estimates. *arXiv*, 2018.
- [34] Mark Ibrahim, Melissa Louie, Ceena Modarres, and John Paisley. Global explanations of neural networks: Mapping the landscape of predictions. *CoRR*, abs/1902.02384, 2019.
- [35] Sérgio Jesus, Catarina Belém, Vladimir Balayan, João Bento, Pedro Saleiro, Pedro Bizarro, and João Gama. How can i choose an explainer? an application-grounded evaluation of post-hoc explanations. In *FAccT*, 2021.
- [36] Kareem L Jordan and Tina L Freiburger. The effect of race/ethnicity on sentencing: Examining sentence type, jail length, and prison length. In *Journal of Ethnicity in Criminal Justice*. Taylor & Francis, 2015.
- [37] Amir-Hossein Karimi, Gilles Barthe, Borja Balle, and Isabel Valera. Model-agnostic counterfactual explanations for consequential decisions. *arXiv*, 2019.
- [38] Amir-Hossein Karimi, Bernhard Schölkopf, and Isabel Valera. Algorithmic recourse: from counterfactual explanations to interventions. *CoRR*, abs/2002.06278, 2020.
- [39] Amir-Hossein Karimi, Julius von Kügelgen, Bernhard Schölkopf, and Isabel Valera. Algorithmic recourse under imperfect causal knowledge: a probabilistic approach. *CoRR*, 2020.
- [40] Harmanpreet Kaur, Harsha Nori, Samuel Jenkins, Rich Caruana, Hanna Wallach, and Jennifer Wortman Vaughan. Interpreting interpretability: Understanding data scientists’ use of interpretability tools for machine learning. In *CHI Conference on Human Factors in Computing Systems*, 2020.
- [41] Joon Sik Kim, Gregory Plumb, and Ameet Talwalkar. Sanity simulations for saliency methods. *arXiv*, 2021.
- [42] Narine Kokhlikyan, Vivek Miglani, Miguel Martin, Edward Wang, Bilal Alsallakh, Jonathan Reynolds, Alexander Melnikov, Natalia Kliushkina, Carlos Araya, Siqi Yan, and Orion Reblitz-Richardson. Captum: A unified and generic model interpretability library for pytorch, 2020.
- [43] Satyapriya Krishna, Tessa Han, Alex Gu, Javin Pombra, Shahin Jabbari, Steven Wu, and Himabindu Lakkaraju. The disagreement problem in explainable machine learning: A practitioner’s perspective. *arXiv*, 2022.
- [44] Isaac Lage, Emily Chen, Jeffrey He, Menaka Narayanan, Been Kim, Sam Gershman, and Finale Doshi-Velez. An evaluation of the human-interpretability of explanation. *arXiv*, 2019.
- [45] Himabindu Lakkaraju and Osbert Bastani. “how do i fool you?” manipulating user trust via misleading black box explanations. In *AAAI Conference on AIES*, 2020.

- [46] Himabindu Lakkaraju, Stephen H Bach, and Jure Leskovec. Interpretable decision sets: A joint framework for description and prediction. In *Proceedings of the 22nd ACM SIGKDD international conference on knowledge discovery and data mining*, pages 1675–1684, 2016.
- [47] Himabindu Lakkaraju, Ece Kamar, Rich Caruana, and Jure Leskovec. Faithful and customizable explanations of black box models. In *Proceedings of the 2019 AAAI/ACM Conference on AI, Ethics, and Society*, pages 131–138, 2019.
- [48] Benjamin Letham, Cynthia Rudin, Tyler H McCormick, and David Madigan. Interpretable classifiers using rules and bayesian analysis: Building a better stroke prediction model. *The Annals of Applied Statistics*, 9(3):1350–1371, 2015.
- [49] Pantelis Linardatos, Vasilis Papastefanopoulos, and Sotiris Kotsiantis. Explainable ai: A review of machine learning interpretability methods. *Entropy*, 23(1):18, 2021.
- [50] Zachary C Lipton. The mythos of model interpretability. *CoRR*, abs/1606.03490, 2016.
- [51] Yang Liu, Sujay Khandagale, Colin White, and Willie Neiswanger. Synthetic benchmarks for scientific research in explainable machine learning. In *NeurIPS Datasets and Benchmarks Track*, 2021.
- [52] Arnaud Looveren and Janis Klaise. Interpretable counterfactual explanations guided by prototypes. *CoRR*, abs/1907.02584, 2019.
- [53] Yin Lou, Rich Caruana, and Johannes Gehrke. Intelligible models for classification and regression. In *KDD*, 2012.
- [54] Scott M Lundberg and Su-In Lee. A unified approach to interpreting model predictions. In I. Guyon, U. V. Luxburg, S. Bengio, H. Wallach, R. Fergus, S. Vishwanathan, and R. Garnett, editors, *Neural Information Processing Systems (NIPS)*, pages 4765–4774. Curran Associates, Inc., 2017.
- [55] Scott M Lundberg and Su-In Lee. A unified approach to interpreting model predictions. In *Advances in Neural Information Processing Systems*, pages 4765–4774, 2017.
- [56] W James Murdoch, Chandan Singh, Karl Kumbier, Reza Abbasi-Asl, and Bin Yu. Definitions, methods, and applications in interpretable machine learning. *Proceedings of the National Academy of Sciences*, 2019.
- [57] Martin Pawelczyk, Klaus Broelemann, and Gjergji Kasneci. Learning model-agnostic counterfactual explanations for tabular data. In *WWW*, 2020.
- [58] Martin Pawelczyk, Sascha Bielawski, Johan Van den Heuvel, Tobias Richter, and Gjergji Kasneci. Carla: A python library to benchmark algorithmic recourse and counterfactual explanation algorithms. In *NeurIPS Benchmark and Datasets Track*, 2021.
- [59] Vitali Petsiuk, Abir Das, and Kate Saenko. Rise: Randomized input sampling for explanation of black-box models. *arXiv*, 2018.
- [60] Forough Poursabzi-Sangdeh, Daniel G Goldstein, Jake M Hofman, Jennifer Wortman Vaughan, and Hanna Wallach. Manipulating and measuring model interpretability. *CoRR*, 2018.
- [61] Rafael Poyiadzi, Kacper Sokol, Raul Santos-Rodriguez, Tijl De Bie, and Peter Flach. FACE: Feasible and actionable counterfactual explanations. In *AAAI Conference on AIES*, 2020.
- [62] Marco Tulio Ribeiro, Sameer Singh, and Carlos Guestrin. "why should i trust you?": Explaining the predictions of any classifier. In *KDD*, 2016.
- [63] Marco Tulio Ribeiro, Sameer Singh, and Carlos Guestrin. Anchors: High-precision model-agnostic explanations. In *AAAI*, 2018.
- [64] Cynthia Rudin. Stop explaining black box machine learning models for high stakes decisions and use interpretable models instead. *Nature Machine Intelligence*, 2019.

- [65] Ramprasaath R Selvaraju, Michael Cogswell, Abhishek Das, Ramakrishna Vedantam, Devi Parikh, and Dhruv Batra. Grad-cam: Visual explanations from deep networks via gradient-based localization. In *ICCV*, 2017.
- [66] Avanti Shrikumar, Peyton Greenside, and Anshul Kundaje. Learning important features through propagating activation differences. In *ICML*, 2017.
- [67] Karen Simonyan, Andrea Vedaldi, and Andrew Zisserman. Deep inside convolutional networks: Visualising image classification models and saliency maps. In *ICLR*, 2014.
- [68] Dylan Slack, Sophie Hilgard, Emily Jia, Sameer Singh, and Himabindu Lakkaraju. Fooling lime and shap: Adversarial attacks on post hoc explanation methods. In *AAAI Conference on AIES*, 2020.
- [69] Dylan Slack, Anna Hilgard, Sameer Singh, and Himabindu Lakkaraju. Reliable post hoc explanations: Modeling uncertainty in explainability. *NeurIPS*, 2021.
- [70] Daniel Smilkov, Nikhil Thorat, Been Kim, Fernanda Viégas, and Martin Wattenberg. Smoothgrad: removing noise by adding noise. *arXiv*, 2017.
- [71] Jack W Smith, James E Everhart, WC Dickson, William C Knowler, and Robert Scott Johannes. Using the adap learning algorithm to forecast the onset of diabetes mellitus. In *Proceedings of the annual symposium on computer application in medical care*, page 261. American Medical Informatics Association, 1988.
- [72] Mukund Sundararajan, Ankur Taly, and Qiqi Yan. Axiomatic attribution for deep networks. In *ICML*, 2017.
- [73] Sohini Upadhyay, Shalmali Joshi, and Himabindu Lakkaraju. Towards robust and reliable algorithmic recourse. *NeurIPS*, 2021.
- [74] Berk Ustun, Alexander Spangher, and Yang Liu. Actionable recourse in linear classification. In *FAccT*, 2019.
- [75] Sahil Verma, John Dickerson, and Keegan Hines. Counterfactual explanations for machine learning: A review. *arXiv*, 2020.
- [76] Sandra Wachter, Brent Mittelstadt, and Chris Russell. Counterfactual explanations without opening the black box: Automated decisions and the GDPR. *Harvard Journal of Law & Technology*, 31:841, 2017.
- [77] Fulton Wang and Cynthia Rudin. Falling rule lists. In *Artificial Intelligence and Statistics*, pages 1013–1022. PMLR, 2015.
- [78] Leanne S Whitmore, Anthe George, and Corey M Hudson. Mapping chemical performance on molecular structures using locally interpretable explanations. *CoRR*, abs/1611.07443, 2016.
- [79] I-Cheng Yeh and Che-hui Lien. The comparisons of data mining techniques for the predictive accuracy of probability of default of credit card clients. In *Expert Systems with Applications*, 2009.
- [80] Jiaming Zeng, Berk Ustun, and Cynthia Rudin. Interpretable classification models for recidivism prediction. *Journal of the Royal Statistical Society: Series A (Statistics in Society)*, 2017.
- [81] Jianlong Zhou, Amir H Gandomi, Fang Chen, and Andreas Holzinger. Evaluating the quality of machine learning explanations: A survey on methods and metrics. *Electronics*, 10(5):593, 2021.

## A Evaluation Metrics

Here, we describe different evaluation metrics that we included in the first iteration of OpenXAI. More specifically, we discuss various metrics (and their implementations) for evaluating the faithfulness, stability, and fairness of explanations generated using a given feature attribution method.

**1) Faithfulness.** To measure how faithfully a given explanation mimics the underlying model, prior work has either leveraged synthetic datasets to obtain ground truth explanations or measured the differences in predictions when feature values are perturbed [59]. Here, we discuss the two broad categories of faithfulness metrics included in OpenXAI, namely ground-truth and predictive faithfulness.

*a) Ground-truth Faithfulness.* OpenXAI leverages the following metrics outlined by Krishna et al. [43] to calculate the agreement between ground-truth explanations (i.e., coefficients of logistic regression models) and explanations generated by state-of-the-art methods.

- *Feature Agreement (FA)* metric computes the fraction of top- $K$  features that are common between a given post hoc explanation and the corresponding ground truth explanation.
- *Rank Agreement (RA)* metric measures the fraction of top- $K$  features that are not only common between a given post hoc explanation and the corresponding ground truth explanation, but also have the same position in the respective rank orders.
- *Sign Agreement (SA)* metric computes the fraction of top- $K$  features that are not only common between a given post hoc explanation and the corresponding ground truth explanation, but also share the same sign (direction of contribution) in both the explanations.
- *Signed Rank Agreement (SRA)* metric computes the fraction of top- $K$  features that are not only common between a given post hoc explanation and the corresponding ground truth explanation, but also share the same feature attribution sign (direction of contribution) and position (rank) in both the explanations.
- *Rank Correlation (RC)* metric computes the Spearman’s rank correlation coefficient to measure the agreement between feature rankings provided by a given post hoc explanation and the corresponding ground truth explanation.
- *Pairwise Rank Agreement (PRA)* metric captures if the relative ordering of every pair of features is the same for a given post hoc explanation as well as the corresponding ground truth explanation i.e., if feature A is more important than B according to one explanation, then the same should be true for the other explanation. More specifically, this metric computes the fraction of feature pairs for which the relative ordering is the same between the two explanations.

**Reported metric values.** While the aforementioned metrics quantify the ground-truth faithfulness of individual explanations, we report a single value corresponding to each explanation method and dataset to facilitate easy comparison of state-of-the-art methods. To this end, we adopt a similar strategy as that of Krishna et al. [43] and compute the aforementioned metrics for each instance in the test data and then average these values. To arrive at the reported values of FA, RA, SA, and SRA metrics, instead of setting a specific value for  $K$ , we do the above computation for all possible values of  $K$  and then plot the different values of  $K$  (on the x-axis) and the corresponding averaged metric values (on the y-axis), and calculate the area under the resulting curve (AUC). On the other hand, in case of RC and PRA metrics, we set  $K$  to the total number of features and compute the averaged metric values (across all test instances) as discussed above.

*b) Predictive Faithfulness.* Following Petsiuk et al. [59], OpenXAI includes two complementary predictive faithfulness metrics: i) Prediction Gap on Important feature perturbation (PGI) which measures the difference in prediction probability that results from perturbing the features deemed as influential by a given post hoc explanation, and ii) Prediction Gap on Unimportant feature perturbation (PGU) which measures the difference in prediction probability that results from perturbing the features deemed as unimportant by a given post hoc explanation.

For a given instance  $\mathbf{x}$ , we first obtain the prediction probability  $\hat{y}$  output by the underlying model  $f$ , i.e.,  $\hat{y} = f(\mathbf{x})$ . Let  $e_{\mathbf{x}}$  be an explanation for the model prediction of  $\mathbf{x}$ . In case of PGU, we then generate a perturbed instance  $\mathbf{x}'$  in the local neighborhood of  $\mathbf{x}$  by holding the top- $k$  features constant, and slightly perturbing the values of all the other features by adding a small amount of Gaussian

noise. In case of PGI, we generate a perturbed instance  $\mathbf{x}'$  in the local neighborhood of  $\mathbf{x}$  by slightly perturbing the values of the top- $k$  features by adding a small amount of Gaussian noise, and holding all the other features constant. Finally, we compute the expected value of the prediction difference between the original and perturbed instances as:

$$\text{PGI}(\mathbf{x}, f, e_{\mathbf{x}}, k) = \mathbb{E}_{\mathbf{x}' \sim \text{perturb}(\mathbf{x}, e_{\mathbf{x}}, \text{top-}K)}[|\hat{y} - f(\mathbf{x}')|], \quad (1)$$

$$\text{PGU}(\mathbf{x}, f, e_{\mathbf{x}}, k) = \mathbb{E}_{\mathbf{x}' \sim \text{perturb}(\mathbf{x}, e_{\mathbf{x}}, \text{non top-}K)}[|\hat{y} - f(\mathbf{x}')|], \quad (2)$$

where  $\text{perturb}(\cdot)$  returns the noisy versions of  $\mathbf{x}$  as described above.

**Reported metric values.** Similar to the ground-truth faithfulness metrics, we report PGI and PGU by calculating the AUC over all values of  $K$ .

**2) Stability.** We leverage the metrics Relative Input Stability (RIS), Relative Representation Stability (RRS), and Relative Output Stability (ROS) [4] which measure the maximum change in explanation relative to changes in the inputs, internal representations learned by the model, and output prediction probabilities respectively. These metrics can be written formally as:

$$\text{RIS} = \frac{\|\mathbf{x}\|_p}{\|e_{\mathbf{x}}\|_p} \max_{\mathbf{x}'} \frac{\|e_{\mathbf{x}} - e_{\mathbf{x}'}\|_p}{\|\mathbf{x} - \mathbf{x}'\|_p}, \quad \forall \mathbf{x}' \text{ s.t. } \mathbf{x}' \in \mathcal{N}_{\mathbf{x}}; \hat{y}_{\mathbf{x}} = \hat{y}_{\mathbf{x}'} \quad (3)$$

where  $\mathcal{N}_{\mathbf{x}}$  is a neighborhood of instances  $\mathbf{x}'$  around  $\mathbf{x}$ , and  $e_{\mathbf{x}}$  and  $e_{\mathbf{x}'}$  denote the explanations corresponding to instances  $\mathbf{x}$  and  $\mathbf{x}'$ , respectively. The numerator of the metric measures the  $l_p$  norm of the percent change of explanation  $e_{\mathbf{x}'}$  on the perturbed instance  $\mathbf{x}'$  with respect to the explanation  $e_{\mathbf{x}}$  on the original point  $\mathbf{x}$ . The denominator measures the  $l_p$  norm between the (normalized) inputs  $\mathbf{x}$  and  $\mathbf{x}'$ , and the max term in the denominator prevents division by zero.

$$\text{RRS} = \frac{\|\mathcal{L}_{\mathbf{x}}\|_p}{\|e_{\mathbf{x}}\|_p} \max_{\mathbf{x}'} \frac{\|e_{\mathbf{x}} - e_{\mathbf{x}'}\|_p}{\|\mathcal{L}_{\mathbf{x}} - \mathcal{L}_{\mathbf{x}'}\|_p}, \quad \forall \mathbf{x}' \text{ s.t. } \mathbf{x}' \in \mathcal{N}_{\mathbf{x}}; \hat{y}_{\mathbf{x}} = \hat{y}_{\mathbf{x}'} \quad (4)$$

where  $\mathcal{L}(\cdot)$  denotes the internal representations learned by the model. Without loss of generality, we use a two layer neural network model in our experiments and use the output of the first layer for computing RRS. Similarly, we can also define ROS as:

$$\text{ROS} = \frac{\|f(\mathbf{x})\|_p}{\|e_{\mathbf{x}}\|_p} \max_{\mathbf{x}'} \frac{\|e_{\mathbf{x}} - e_{\mathbf{x}'}\|_p}{\|f(\mathbf{x}) - f(\mathbf{x}')\|_p}, \quad \forall \mathbf{x}' \text{ s.t. } \mathbf{x}' \in \mathcal{N}_{\mathbf{x}}; \hat{y}_{\mathbf{x}} = \hat{y}_{\mathbf{x}'}, \quad (5)$$

where  $f(\mathbf{x})$  and  $f(\mathbf{x}')$  are the output prediction probabilities for  $\mathbf{x}$  and  $\mathbf{x}'$ , respectively. To the best of our knowledge, OpenXAI is the first benchmark to incorporate all the above stability metrics.

**Reported metric values..** We compute the aforementioned metrics for each instance in the test set, and then average these values.

**3) Fairness.** It is important to ensure that there are no significant disparities between the reliability of post hoc explanations corresponding to instances in the majority and the minority subgroups. To this end, we average all the aforementioned metric values across instances in the majority and minority subgroups, and then compare the two estimates to check if there are significant disparities [18]. See Figures 1 to 2 for logistic regression models, and Figures 3 to 4 for neural network models.

## B Additional Related Work

Our work builds on the vast literature on model interpretability and explainability. Below is an overview of additional works that were not included in Section 1 due to space constraints.

**Inherently Interpretable Models and Post hoc Explanations.** Many approaches learn inherently interpretable models such as rule lists [80, 77], decision trees and decision lists [48], and others [46, 13, 53, 15]. However, complex models such as deep neural networks often achieve higher accuracy than simpler models [62]. Thus, there has been significant interest in constructing post hoc explanations to understand their behavior. To this end, several techniques have been proposed in

recent literature to construct *post hoc explanations* of complex decision models. For instance, LIME, SHAP, Anchors, BayesLIME, and BayesSHAP [62, 55, 63, 69] are considered *perturbation-based local* explanation methods because they leverage perturbations of individual instances to construct interpretable local approximations (e.g., linear models). On the other hand, methods such as Vanilla Gradients, Gradient x Input, SmoothGrad, Integrated Gradients, and GradCAM [67, 72, 65, 70] are referred to as *gradient-based local* explanation methods since they leverage gradients computed with respect to input features of individual instances to explain individual model predictions.

There has also been recent work on constructing *counterfactual explanations* which capture what changes need to be made to a given instance in order to flip its prediction [76, 74, 37, 61, 52, 11, 38, 57, 39, 58]. Such explanations can be leveraged to provide recourse to individuals negatively impacted by algorithmic decisions. An alternate class of methods referred to as *global* explanation methods attempt to summarize the behavior of black-box models as a whole rather than in relation to individual data points [47, 12]. A more detailed treatment of this topic is provided in other comprehensive survey articles [8, 30, 56, 49, 17].

In this work, we focus primarily on *local feature attribution-based post hoc explanation methods* i.e., explanation methods which attempt to explain individual model predictions by outputting a vector of feature importances. More specifically, the goal of this work is to enable systematic benchmarking of these methods in an efficient and transparent manner.

**Evaluating Post hoc Explanations.** In addition to the quantitative metrics designed to evaluate the *reliability* of post hoc explanation methods [51, 81, 7, 18] (See Section 1), prior works have also introduced *human-grounded* approaches to evaluate the *interpretability* of explanations generated by these methods [21]. For example, Lakkaraju and Bastani [45] carry out a user study to understand if misleading explanations can fool domain experts into deploying racially biased models, while Kaur et al. [40] find that explanations are often over-trusted and misused. Similarly, Poursabzi-Sangdeh et al. [60] find that supposedly-interpretable models can lead to a decreased ability to detect and correct model mistakes, possibly due to information overload. Jesus et al. [35] introduce a method to compare explanation methods based on how subject matter experts perform on specific tasks with the help of explanations. Lage et al. [44] use insights from rigorous human-subject experiments to inform regularizers used in explanation algorithms. In contrast to the aforementioned research, our work leverages twenty-two different state-of-the-art quantitative metrics to systematically benchmark the reliability (and not interpretability) of post hoc explanation methods.

**Limitations and Vulnerabilities of Post hoc Explanations.** Various quantitative metrics proposed in literature (See Section 1) were also leveraged to analyze the behavior of post hoc explanation methods and their vulnerabilities—e.g., Ghorbani et al. [29] and Slack et al. [68] demonstrated that methods such as LIME and SHAP may result in explanations that are not only inconsistent and unstable, but also prone to adversarial attacks. Furthermore Lakkaraju and Bastani [45] and Slack et al. [68] showed that explanations which do not accurately represent the importance of sensitive attributes (e.g., race, gender) could potentially mislead end users into believing that the underlying models are fair when they are not [45, 68, 6]. This, in turn, could lead to the deployment of unfair models in critical real world applications. There is also some discussion about whether models which are not inherently interpretable ought to be used in high-stakes decisions at all. Rudin [64] argues that post hoc explanations tend to be unfaithful to the model to the extent that their usefulness is severely compromised. While this line of work demonstrates different ways in which explanations could potentially induce inaccuracies and biases in real world applications, they do not focus on systematic benchmarking of post hoc explanation methods which is the main goal of our work.

## C Synthetic Dataset

Our proposed data generation process described in Algorithm 1 is designed to encapsulate arbitrary feature dependencies, unambiguous definitions of local neighborhoods, and clear descriptions of feature influences. In our algorithm 1, the local neighborhood of a sample is controlled by its cluster membership  $k$ , while the degree of feature dependency can be easily controlled by the user setting  $\Sigma_k$  to desired values. The default value of  $\Sigma_k = \mathbf{I}$ , where  $\mathbf{I}$  is the identity matrix, indicating that all features are independent of one another. The elements of the true underlying weight vector  $w_k$  are sampled from a uniform distribution:  $w_k \sim \mathcal{U}(l, u)$ . We set  $l = -1$  and  $u = 1$ . The masking vectors  $m_k$  with elements  $m_{k,j}$  are generated by a Bernoulli distribution:  $m_{k,j} \sim \mathcal{B}(p)$ , where the parameter



$p$  controls the ground-truth explanation sparsity. We set  $p = 0.25$ . Further, the cluster centers are chosen as follows: when the number of features  $d$  is smaller than or equal to the number of clusters  $K$ , then we set the first cluster center to  $[1, 0, \dots, 0]$ , the second one to  $[0, 1, \dots, 0]$ , etc. We also introduce a multiplier  $\kappa$  to control the distance between the cluster centers so that the cluster centers are located at  $\mu_1 = \kappa \cdot [1, 0, \dots, 0]$ ,  $\mu_2 = \kappa \cdot [0, 1, \dots, 0]$ , etc. We set  $\kappa = 6$ . In general, we have observed that lower values of  $\kappa$  result in more complex classification problems. When the number of features  $d$  is greater than the number of clusters  $K$ , we adjust the above described approach slightly: we first compute  $\ell = \lfloor K/d \rfloor$ , and then we compute the cluster centers for the first  $d$  clusters as described above, for the next  $d$  clusters we use  $\mu_{d+1} = 2\kappa \cdot [1, 0, \dots, 0]$ ,  $\mu_{d+2} = 2\kappa \cdot [0, 1, \dots, 0]$ , etc. If  $\ell = 1$ , we stop this procedure here, else we continue, and repeat filling up the clusters  $\mu_{2d+1} = 3\kappa \cdot [1, 0, \dots, 0]$ ,  $\mu_{2d+2} = 3\kappa \cdot [0, 1, \dots, 0]$ , etc.

---

**Algorithm 1: SYNTHGAUSS**


---

**input** : number of clusters:  $K$ , cluster centers:  $[\mu_1, \mu_2, \dots, \mu_K]$ , cluster variances:  $[\Sigma_1, \dots, \Sigma_K]$ , Weight vectors:  $[w_1, \dots, w_K]$ , masking vectors:  $[m_1, \dots, m_K]$   
**output** : features:  $\mathbf{X}$ , labels:  $\mathbf{y}$   
 $\mathbf{X} = \mathbf{0}_{n \times d}$  ;  
 $\Pi = \mathbf{0}_{n \times 1}$  ;  
**for**  $i = 1:n$  **do**  
     $k \leftarrow \text{Cat}(K)$  # Randomly picks a cluster index ;  
     $x_i \sim \mathcal{N}(\mu_k, \Sigma_k)$  # Samples Gaussian instance ;  
     $\mathbf{X}[i, :] = x_i$  ;  
     $\pi_1 = \mathbb{P}(y_i = 1 | \mathbf{x}_i) = \frac{\exp((w_k \odot m_k)^\top x_i)}{1 + \exp((w_k \odot m_k)^\top x_i)}$  # Get class probability ;  
     $\Pi[i] = \pi_1$  ;  
 $\tilde{\pi} = \text{get\_median}(\Pi)$  ;  
**for**  $i = 1:n$  **do**  
     $y_i = \mathbb{I}(\Pi[i] > \tilde{\pi})$  # Make sure classes are balanced ;  
**Return**:  $\mathbf{X}, \mathbf{y}$  ;

---

**Theorem 1** *If a given dataset encapsulates the properties of feature independence, unambiguous and well-separated local neighborhoods, and a unique ground truth explanation for each local neighborhood, the most accurate model trained on such a dataset will adhere to the unique ground truth explanation of each local neighborhood.*

*Proof:* Before we describe the proof, we begin by first formalizing the properties of feature independence, unambiguous and well-separated local neighborhoods, and a unique ground truth explanation for each local neighborhood using some notation. Let  $A = [a_1, a_2, \dots, a_d]$  denote the vector of input features in a given dataset  $D$ , and let the instances in the dataset  $D$  be separated into  $K$  clusters (local neighborhoods) based on their proximity.

**Feature independence:** The dataset  $D$  satisfies feature independence if  $P(a_i | a_j) = P(a_i) \forall i, j \in \{1, 2, \dots, d\}$  and  $i \neq j$ .

**Unambiguous and well-separated local neighborhoods:** The dataset  $D$  is said to constitute unambiguous and well-separated local neighborhoods if  $\text{dist}(x_{i,j}, x_{p,q}) \gg \text{dist}(x_{i,j}, x_{i,l}) \forall i, p \in \{1, 2, \dots, K\}$  where  $x_{i,j}$  and  $x_{i,l}$  are the  $j^{\text{th}}$  and  $l^{\text{th}}$  instances of some cluster  $i$ ,  $x_{p,q}$  is the  $q^{\text{th}}$  instance of cluster  $p$  and  $p \neq i$ . The above implies that the distances between points in different clusters should be significantly higher than the distances between points in the same cluster.

**Unique ground truth explanation for each local neighborhood:** The dataset  $D$  is said to comprise of unique ground truth explanations for each local neighborhood if the ground truth labels of instances in each cluster  $k \in \{1, 2, \dots, K\}$  are generated as a function of a subset of features  $A_k \subseteq A$  where there is a clear relative ordering among features in  $A_k$  which is captured by the weight vector  $w_k$ , and features in  $A$  are completely independent of each other. [Note that the influential feature set  $A_k$  corresponding to the cluster  $k$  is also captured using the mask vector  $m_k$  (See Section 2) where  $m_{k,i} = 1$  if the  $i^{\text{th}}$  feature is in set  $A_k$ ]. This would imply that there is a clear description of the top- $T$  features (and their relative ordering) where  $T \leq |A_k|$  influence the ground truth labeling process.

With the above information in place, let us now consider a model  $\mathcal{M}$  which is trained on the dataset  $D$  and achieves highest possible accuracy on it. To show that this model indeed adheres to the unique ground truth explanations of each of the local neighborhoods (clusters), we adopt the strategy of proof by contradiction. To this end, we begin with the assumption that the model  $\mathcal{M}$  does not adhere to the unique ground truth explanation of some local neighborhood  $k \in \{1, 2, \dots, K\}$  i.e., the top- $T$  features leveraged by model  $\mathcal{M}$  for instances in cluster  $k$  (denoted by  $\mathcal{M}_T^k$ ) do not exactly match the top- $T$  features leveraged by the ground truth labeling process where  $T \leq |A_k|$ . This happens either when there is a mismatch in the relative ordering among the top- $T$  features used by the model  $\mathcal{M}$  and the ground truth labeling process (or) when there is at least one feature  $a$  that appears among the top- $T$  features used by the model but not the ground truth labeling process. In either case, we can construct another model  $\mathcal{M}'$  such that the top- $T$  features used by  $\mathcal{M}'$  match the top- $T$  features of the ground truth labeling process exactly, and the accuracy of  $\mathcal{M}'$  will be higher than that of  $\mathcal{M}$ . This contradicts the assumption that the model  $\mathcal{M}$  has the highest possible accuracy, thus demonstrating that the model with highest possible accuracy would adhere to the unique ground truth explanation of each local neighborhood.

## D Benchmarking Analysis

### D.1 Real-World Datasets

In addition to the synthetic dataset, the OpenXAI library includes seven real-world benchmark datasets from high-stakes domains. Table 1 provides a summary of the real-world datasets currently included in OpenXAI. Our library implements multiple data split strategies and allows users to customize the percentages of train-test splits. To this end, if a given dataset comes with a pre-determined train and test splits, OpenXAI loads the training and testing dataloaders from those pre-determined splits. Otherwise, OpenXAI’s dataloader divides the entire dataset randomly into train (80%) and test (20%). Next, we detail the covariates  $\mathbf{x}$  and labels  $\mathbf{y}$  for each dataset.

**German Credit** [22] The dataset comprises of demographic (age, gender), personal (marital status), and financial (income, credit duration) features from 1,000 credit applicants, where they are categorized into good vs. bad customer depending on their credit risk.

**HELOC** [25] The dataset comprises of financial (e.g., total number of trades, average credit months in file) attributes from anonymized applications submitted by 9,871 real homeowners. A HELOC (Home Equity Line of Credit) is a line of credit typically offered by a bank as a percentage of home equity. The fundamental task is to use the information about the applicant in their credit report to predict whether they will repay their HELOC account within 2 years.

**Adult Income** [79] The dataset contains demographic (e.g., age, race, and gender), education (degree), employment (occupation, hours-per week), personal (marital status, relationship), and financial (capital gain/loss) features for 45,222 individuals. The task is to predict whether an individual’s income exceeds \$50K per year vs. not.

**COMPAS** [36] The dataset has criminal records and demographics features for 6,172 defendants released on bail at U.S state courts during 1990-2009. The task is to classify defendants into bail (i.e., unlikely to commit a violent crime if released) vs. no bail (i.e., likely to commit a violent crime).

**Give Me Some Credit** [27] The dataset incorporates demographic (age), personal (number of dependents), and financial (e.g., monthly income, debt ratio, etc.) features for 102,209 individuals. The task is to predict the probability whether or not a customer will experience financial distress in the next two years. The aim of the dataset is to build models that customers can use to the best financial decisions.

We also include the **Pima-Indians Diabetes** [71] and **Framingham Heart Study** [1] datasets (see Appendix D.5).

### D.2 Explanation Methods

OpenXAI provides implementations for six explanation methods: Vanilla Gradients [67], Integrated Gradients [72], SmoothGrad [70], Gradient x Input [66], LIME [62], and SHAP [55]. Table 6 summarizes how these methods differ along two axes: whether each method requires “White-box

Access” to model gradients and whether each method learns a local approximation model to generate explanations.

**Table 6:** Summary of currently available feature attribution methods in OpenXAI. “Learning?” denotes whether learning/training procedures are required to generate explanations and “White-box Access?” denotes if the access to the internals of the model (e.g., gradients) are needed.

Method	Learning?	White-box Access?
Random	✗	✗
VanillaGrad	✗	✓
IntegratedGrad	✗	✓
Gradient x Input	✗	✓
SmoothGrad	✗	✓
SHAP	✓	✗
LIME	✓	✗

**Implementations.** We used existing public implementations of all explanation methods in our experiments. We used the following captum software package classes: i) `captum.attr.Saliency` for Vanilla Gradients; ii) `captum.attr.IntegratedGradients` for Integrated Gradients; iii) `captum.attr.NoiseTunnel` and `captum.attr.Saliency` for SmoothGrad; iv) `captum.attr.InputXGradient` for Gradient x Input; and v) `captum.attr.KernelShap` for SHAP. Finally, we use the authors’ python package for LIME.

### D.3 Hyperparameter details

OpenXAI uses default hyperparameter settings for all explanation methods following the authors’ guidelines. Every explanation method has a corresponding parameter dictionary that stores all the default parameter values. Below, we detail the hyperparameters of individual explanation methods used in our experiments. Seed is set to 0 for all explanation methods to allow reproducibility.

**a) `params_lime`** = {`‘seed’`: 0, `‘lime_mode’`: `‘tabular’`, `‘sample_around_instance’`: True, `‘kernel_width’`: 0.75, `‘n_samples’`: 1000, `‘discretize_continuous’`: False, `‘std’`: 0.1}

*Description.* The option `‘tabular’` indicates that we wish to compute explanations on a tabular data set. The option `‘lime_sample_around_instance’` makes sure that the sampling is conducted in a local neighborhood around the point that we wish to explain. The `‘lime_discretize_continuous’` option ensures that continuous variables are kept continuous, and are not discretized. This parameter sets the `‘lime_standard_deviation’` of the Gaussian random variable that is used to sample around the instance that we wish to explain. We set this to a small value, ensuring that we in fact sample from a local neighborhood.

**b) `params_shap`** = {`‘seed’`: 0, `‘n_samples’`: 500, `‘model_impl’`: `‘torch’`}

*Description.* The parameter `‘shap_n_samples’` controls the number of samples of the original model used to train the surrogate SHAP model, while the parameter `‘model_impl’` toggles between models from `‘torch’` and `‘sklearn’`.

**c) `params_grads`** = {`‘absolute_value’`: False}

*Description.* The parameter `‘grad_absolute_value’` controls whether the absolute value of each element in the explanation vector should be taken or not.

**d) `params_sg`** = {`‘n_samples’`: 500, `‘standard_deviation’`: 0.1}

*Description.* The parameter `‘sg_n_samples’` sets the number of samples used in the Gaussian random variable to smooth the gradient, while `‘sg_standard_deviation’` determines the size of the local neighborhood the Gaussian random variables are sampled from. We use a small value, ensuring that we sample from a local neighborhood.

**e) `params_ig`** = {`‘method’`: `‘gausslegendre’`, `‘multiply_by_inputs’`: False}

Further, we parameterized our data-generating process as follows.

**f) `params_gauss`** = {`‘n_samples’`: 1000, `‘dim’`: 20, `‘n_clusters’`: 10, `‘distance_to_center’`: 6, `‘test_size’`: 0.25, `‘upper_weight’`: 1, `‘lower_weight’`: -1, `‘seed’`: 564, `‘sigma’`: None, `‘sparsity’`: 0.25}

*Description.* The above parameters can be matched with the parameters from the data generating process described in Appendix C: in particular, ‘sparsity’ =  $p$ , ‘upper\_weight’ =  $u$ , ‘lower\_weight’ =  $l$ , ‘dim’ =  $d$ , ‘n\_clusters’ =  $K$ , ‘distance\_to\_center’ =  $\kappa$  and ‘sigma’=None implies that the identity matrix is used, i.e.,  $\Sigma_k = \mathbf{I}$ .

In addition, for a given instance  $\mathbf{x}$ , some evaluation metrics leverage a perturbation class to generate perturbed samples  $\mathbf{x}'$ . We have a parameterized version of this perturbation class in OpenXAI with the following default parameters:

**g) params\_perturb** = {‘perturbation\_mean’ : 0.0, ‘perturbation\_std’ : 0.05, ‘perturbation\_flip\_percentage’ : 0.03}

Finally, we dynamically infer the top- $k$  value from the input parameter  $k$  and the total number of features,  $d$ , as follows: top- $k = k$  for  $\{k \in \mathbb{Z} \mid 1 \leq k \leq d\}$ ; top- $k = d$  for  $k = -1$ ; and top- $k = \lceil k \times d \rceil$  for  $\{k \in \mathbb{R} \mid 0 < k < 1\}$ .

For predictive faithfulness, we set  $\sigma=0.1$ , and sample 100 perturbations. The flip percentage is set to  $\sigma\sqrt{2/\pi}$  in all cases, which leads to the same expected magnitude of change between continuous and discrete variables when drawing from a Normal distribution. For stability, we set  $\sigma=10^{-5}$ , and sample 1000 points before selecting a subset of 100 samples that share the original input’s prediction.

The  $p$  norm for all stability metrics is set to 2. Seed is set to the special case of -1 for our evaluation metrics, which assumes the index of the specific test instance being evaluated as the seed being used. All default hyperparameters used in our experiments can also be found in the `experiment_config.json` file of our OpenXAI GitHub repository.

#### D.4 Model details

Our current release of OpenXAI has two pre-trained models: i) a logistic regression model and ii) a deep neural network model for all datasets. To support systematic, reproducible, and efficient benchmarking of post hoc explanation methods, we provide the model weights for both models trained on all eight datasets in our pipeline. For neural network models, we use two fully connected hidden layers with 100 nodes in each layer, with ReLU activation functions and an output softmax layer for all datasets. We train both models for 100 epochs using an Adam optimizer with a learning rate of  $\eta=0.001$ . We use min-max scaling to normalize train/test splits, along with dataset-specific batch sizes/positive class weights (to balance the loss function). The best epoch in terms of test accuracy is selected, excluding an initial warmup phase of 5 epochs, and provided that dataset-specific bounds are not exceeded for the proportion of the majority class predicted. Next, we show the performance of both models on all eight datasets.

**Table 7: Results of the machine learning models trained on eight datasets.** Shown are the test accuracies of LR and ANN models. Values corresponding to best performance are bolded.

Dataset	LR	ANN
Synthetic Data	81.76%	<b>90.32%</b>
German Credit	<b>64.00%</b>	61.50%
HELOC	72.35%	<b>73.92%</b>
COMPAS	<b>85.26%</b>	85.02%
Adult Income	83.25%	<b>84.62%</b>
Give Me Some Credit	<b>93.79%</b>	93.43%
Pima-Indians Diabetes	69.48%	<b>77.92%</b>
Framingham Heart Study	80.19%	<b>80.87%</b>

#### D.5 Results for Pima-Indians Diabetes and Framingham Heart Study datasets

We include two new datasets from the healthcare domain and benchmark state-of-the-art explanation methods on these datasets. More specifically, we include the **Pima-Indians Diabetes** [71] and **Framingham Heart Study** [1] datasets both of which have been utilized in recent XAI research. New results with these datasets are shown below. We observe similar insights with these new datasets: predictive faithfulness results are shown in Tables 8-11 below; stability results are shown in Tables 12-15 below.

**Table 8: Ground-truth and predictive faithfulness results on the Pima Indians Diabetes dataset for all explanation methods with LR model.** Shown are average and standard error metric values computed across 1000 test instances.  $\uparrow$  indicates that higher values are better, and  $\downarrow$  indicates that lower values are better. Values corresponding to best performance are bolded.

Method	PRA ( $\uparrow$ )	RC ( $\uparrow$ )	FA ( $\uparrow$ )	RA ( $\uparrow$ )	SA ( $\uparrow$ )	SRA ( $\uparrow$ )	PGU ( $\downarrow$ )	PGI ( $\uparrow$ )
Random	0.470 $\pm$ 0.01	-0.076 $\pm$ 0.03	0.154 $\pm$ 0.02	0.109 $\pm$ 0.02	0.075 $\pm$ 0.02	0.054 $\pm$ 0.01	0.031 $\pm$ 0.00	0.013 $\pm$ 0.00
VanillaGrad	<b>1.000</b> $\pm$ 0.00	<b>1.000</b> $\pm$ 0.00	<b>1.000</b> $\pm$ 0.00	<b>1.000</b> $\pm$ 0.00	<b>1.000</b> $\pm$ 0.00	<b>1.000</b> $\pm$ 0.00	<b>0.026</b> $\pm$ 0.00	<b>0.021</b> $\pm$ 0.00
IntegratedGrad	<b>1.000</b> $\pm$ 0.00	<b>1.000</b> $\pm$ 0.00	<b>1.000</b> $\pm$ 0.00	<b>1.000</b> $\pm$ 0.00	<b>1.000</b> $\pm$ 0.00	<b>1.000</b> $\pm$ 0.00	<b>0.026</b> $\pm$ 0.00	<b>0.021</b> $\pm$ 0.00
Gradient x Input	0.492 $\pm$ 0.01	-0.047 $\pm$ 0.03	0.195 $\pm$ 0.02	0.133 $\pm$ 0.02	0.195 $\pm$ 0.02	0.133 $\pm$ 0.02	0.030 $\pm$ 0.00	0.015 $\pm$ 0.00
SmoothGrad	<b>1.000</b> $\pm$ 0.00	<b>1.000</b> $\pm$ 0.00	<b>1.000</b> $\pm$ 0.00	<b>1.000</b> $\pm$ 0.00	<b>1.000</b> $\pm$ 0.00	<b>1.000</b> $\pm$ 0.00	<b>0.026</b> $\pm$ 0.00	<b>0.021</b> $\pm$ 0.00
SHAP	0.488 $\pm$ 0.01	-0.047 $\pm$ 0.03	0.195 $\pm$ 0.02	0.135 $\pm$ 0.02	0.195 $\pm$ 0.02	0.135 $\pm$ 0.02	0.030 $\pm$ 0.00	0.015 $\pm$ 0.00
LIME	0.980 $\pm$ 0.00	0.986 $\pm$ 0.00	0.985 $\pm$ 0.00	0.985 $\pm$ 0.00	0.985 $\pm$ 0.00	0.985 $\pm$ 0.00	<b>0.026</b> $\pm$ 0.00	<b>0.021</b> $\pm$ 0.00

**Table 9: Ground-truth and predictive faithfulness results on the Framingham Heart dataset for all explanation methods with LR model.** Shown are average and standard error metric values computed across 1000 test instances.  $\uparrow$  indicates that higher values are better, and  $\downarrow$  indicates that lower values are better. Values corresponding to best performance are bolded.

Method	PRA ( $\uparrow$ )	RC ( $\uparrow$ )	FA ( $\uparrow$ )	RA ( $\uparrow$ )	SA ( $\uparrow$ )	SRA ( $\uparrow$ )	PGU ( $\downarrow$ )	PGI ( $\uparrow$ )
Random	0.495 $\pm$ 0.00	-0.013 $\pm$ 0.01	0.168 $\pm$ 0.01	0.067 $\pm$ 0.01	0.090 $\pm$ 0.01	0.040 $\pm$ 0.00	0.086 $\pm$ 0.00	0.025 $\pm$ 0.00
VanillaGrad	<b>1.000</b> $\pm$ 0.00	<b>1.000</b> $\pm$ 0.00	<b>1.000</b> $\pm$ 0.00	<b>1.000</b> $\pm$ 0.00	<b>1.000</b> $\pm$ 0.00	<b>1.000</b> $\pm$ 0.00	<b>0.074</b> $\pm$ 0.00	<b>0.042</b> $\pm$ 0.00
IntegratedGrad	<b>1.000</b> $\pm$ 0.00	<b>1.000</b> $\pm$ 0.00	<b>1.000</b> $\pm$ 0.00	<b>1.000</b> $\pm$ 0.00	<b>1.000</b> $\pm$ 0.00	<b>1.000</b> $\pm$ 0.00	<b>0.074</b> $\pm$ 0.00	<b>0.042</b> $\pm$ 0.00
Gradient x Input	0.619 $\pm$ 0.00	0.280 $\pm$ 0.01	0.472 $\pm$ 0.01	0.313 $\pm$ 0.01	0.472 $\pm$ 0.01	0.313 $\pm$ 0.01	0.089 $\pm$ 0.00	0.029 $\pm$ 0.00
SmoothGrad	<b>1.000</b> $\pm$ 0.00	<b>1.000</b> $\pm$ 0.00	<b>1.000</b> $\pm$ 0.00	<b>1.000</b> $\pm$ 0.00	<b>1.000</b> $\pm$ 0.00	<b>1.000</b> $\pm$ 0.00	<b>0.074</b> $\pm$ 0.00	<b>0.042</b> $\pm$ 0.00
SHAP	0.573 $\pm$ 0.00	0.208 $\pm$ 0.01	0.475 $\pm$ 0.01	0.321 $\pm$ 0.01	0.475 $\pm$ 0.01	0.321 $\pm$ 0.01	0.089 $\pm$ 0.00	0.029 $\pm$ 0.00
LIME	0.978 $\pm$ 0.00	0.991 $\pm$ 0.00	0.971 $\pm$ 0.00	0.951 $\pm$ 0.00	0.971 $\pm$ 0.00	0.951 $\pm$ 0.00	<b>0.074</b> $\pm$ 0.00	<b>0.042</b> $\pm$ 0.00

**Table 10: Predictive faithfulness results on the Pima Indians Diabetes dataset for all explanation methods with ANN model.** Shown are average and standard error metric values computed across 1000 test instances.  $\uparrow$  indicates that higher values are better, and  $\downarrow$  indicates that lower values are better. Values corresponding to best performance are bolded.

Method	PGU ( $\downarrow$ )	PGI ( $\uparrow$ )
Random	0.084 $\pm$ 0.008	0.034 $\pm$ 0.004
VanillaGrad	0.055 $\pm$ 0.006	<b>0.074</b> $\pm$ 0.007
IntegratedGrad	0.055 $\pm$ 0.006	<b>0.074</b> $\pm$ 0.007
Gradient x Input	0.058 $\pm$ 0.006	0.070 $\pm$ 0.007
SmoothGrad	<b>0.054</b> $\pm$ 0.006	<b>0.074</b> $\pm$ 0.007
SHAP	0.069 $\pm$ 0.007	0.056 $\pm$ 0.006
LIME	<b>0.054</b> $\pm$ 0.006	<b>0.074</b> $\pm$ 0.007

**Table 12: Stability results on the Pima Indians Diabetes dataset for all explanation methods with LR model.** Shown are log average and standard error metric values computed across 1000 test instances.  $\uparrow$  indicates that higher values are better, and  $\downarrow$  indicates that lower values are better. Values corresponding to best performance are bolded.

Method	RIS ( $\downarrow$ )	ROS ( $\downarrow$ )
Random	11.86 $\pm$ 0.02	13.11 $\pm$ 0.04
VanillaGrad	-1.01 $\pm$ 0.06	-2.04 $\pm$ 0.08
IntegratedGrad	<b>-2.12</b> $\pm$ 0.06	<b>-3.20</b> $\pm$ 0.08
Gradient x Input	0.70 $\pm$ 0.02	2.75 $\pm$ 0.10
SmoothGrad	6.81 $\pm$ 0.06	7.52 $\pm$ 0.08
SHAP	6.72 $\pm$ 0.04	7.77 $\pm$ 0.08
LIME	7.17 $\pm$ 0.02	8.37 $\pm$ 0.05

**Table 11: Predictive faithfulness results on the Framingham Heart dataset for all explanation methods with ANN model.** Shown are average and standard error metric values computed across 1000 test instances.  $\uparrow$  indicates that higher values are better, and  $\downarrow$  indicates that lower values are better. Values corresponding to best performance are bolded.

Method	PGU ( $\downarrow$ )	PGI ( $\uparrow$ )
Random	0.130 $\pm$ 0.005	0.047 $\pm$ 0.003
VanillaGrad	<b>0.110</b> $\pm$ 0.005	<b>0.089</b> $\pm$ 0.004
IntegratedGrad	0.112 $\pm$ 0.005	0.085 $\pm$ 0.004
Gradient x Input	0.118 $\pm$ 0.005	0.079 $\pm$ 0.004
SmoothGrad	<b>0.110</b> $\pm$ 0.005	0.088 $\pm$ 0.004
SHAP	0.121 $\pm$ 0.005	0.073 $\pm$ 0.004
LIME	<b>0.110</b> $\pm$ 0.005	0.088 $\pm$ 0.004

**Table 13: Stability results on the Framingham Heart dataset for all explanation methods with LR model.** Shown are log average and standard error metric values computed across 1000 test instances.  $\uparrow$  indicates that higher values are better, and  $\downarrow$  indicates that lower values are better. Values corresponding to best performance are bolded.

Method	RIS ( $\downarrow$ )	ROS ( $\downarrow$ )
Random	11.76 $\pm$ 0.01	15.47 $\pm$ 0.02
VanillaGrad	1.25 $\pm$ 0.02	0.80 $\pm$ 0.04
IntegratedGrad	<b>0.43</b> $\pm$ 0.01	<b>-0.30</b> $\pm$ 0.02
Gradient x Input	1.41 $\pm$ 0.01	3.55 $\pm$ 0.08
SmoothGrad	8.59 $\pm$ 0.01	11.22 $\pm$ 0.03
SHAP	9.64 $\pm$ 0.01	11.73 $\pm$ 0.02
LIME	8.95 $\pm$ 0.01	10.67 $\pm$ 0.02

**Table 14: Stability results on the Pima Indians Diabetes dataset for all explanation methods with ANN model.** Shown are log average and standard error metric values computed across 1000 test instances.  $\uparrow$  indicates that higher values are better, and  $\downarrow$  indicates that lower values are better. Values corresponding to best performance are bolded.

Method	RIS ( $\downarrow$ )	RRS ( $\downarrow$ )	ROS ( $\downarrow$ )
Random	11.86 $\pm$ 0.02	11.90 $\pm$ 0.01	15.06 $\pm$ 0.10
VanillaGrad	4.37 $\pm$ 0.70	4.54 $\pm$ 0.76	8.42 $\pm$ 0.99
IntegratedGrad	<b>1.95</b> $\pm$ 0.19	<b>1.93</b> $\pm$ 0.22	<b>2.91</b> $\pm$ 0.15
Gradient x Input	4.59 $\pm$ 0.76	4.77 $\pm$ 0.80	8.72 $\pm$ 0.99
SmoothGrad	10.85 $\pm$ 0.09	10.93 $\pm$ 0.08	13.83 $\pm$ 0.10
SHAP	10.31 $\pm$ 0.04	10.36 $\pm$ 0.04	13.36 $\pm$ 0.16
LIME	10.83 $\pm$ 0.11	11.02 $\pm$ 0.12	13.94 $\pm$ 0.15

**Table 15: Stability results on the Framingham Heart dataset for all explanation methods with ANN model.** Shown are log average and standard error metric values computed across 1000 test instances.  $\uparrow$  indicates that higher values are better, and  $\downarrow$  indicates that lower values are better. Values corresponding to best performance are bolded.

Method	RIS ( $\downarrow$ )	RRS ( $\downarrow$ )	ROS ( $\downarrow$ )
Random	11.76 $\pm$ 0.01	11.25 $\pm$ 0.01	15.21 $\pm$ 0.05
VanillaGrad	5.06 $\pm$ 0.17	4.19 $\pm$ 0.16	<b>4.50</b> $\pm$ 0.37
IntegratedGrad	<b>4.11</b> $\pm$ 0.17	<b>3.23</b> $\pm$ 0.21	5.34 $\pm$ 0.33
Gradient x Input	5.09 $\pm$ 0.18	4.21 $\pm$ 0.17	4.87 $\pm$ 0.29
SmoothGrad	26.14 $\pm$ 0.30	25.94 $\pm$ 0.29	26.77 $\pm$ 0.31
SHAP	16.77 $\pm$ 0.32	16.41 $\pm$ 0.31	19.49 $\pm$ 0.29
LIME	26.56 $\pm$ 0.48	26.52 $\pm$ 0.47	27.43 $\pm$ 0.47

## D.6 Remaining Results on LR models

**Table 16: Ground-truth and predictive faithfulness results on the Synthetic dataset for all explanation methods with LR model.** Shown are average and standard error metric values computed across 1000 test instances.  $\uparrow$  indicates that higher values are better, and  $\downarrow$  indicates that lower values are better. Values corresponding to best performance are bolded.

Method	PRA ( $\uparrow$ )	RC ( $\uparrow$ )	FA ( $\uparrow$ )	RA ( $\uparrow$ )	SA ( $\uparrow$ )	SRA ( $\uparrow$ )	PGU ( $\downarrow$ )	PGI ( $\uparrow$ )
Random	0.503 $\pm$ 0.00	0.008 $\pm$ 0.01	0.155 $\pm$ 0.00	0.052 $\pm$ 0.00	0.078 $\pm$ 0.00	0.027 $\pm$ 0.00	0.122 $\pm$ 0.00	0.047 $\pm$ 0.00
VanillaGrad	<b>1.000</b> $\pm$ 0.00	<b>1.000</b> $\pm$ 0.00	<b>1.000</b> $\pm$ 0.00	<b>1.000</b> $\pm$ 0.00	<b>1.000</b> $\pm$ 0.00	<b>1.000</b> $\pm$ 0.00	<b>0.090</b> $\pm$ 0.00	<b>0.096</b> $\pm$ 0.00
IntegratedGrad	<b>1.000</b> $\pm$ 0.00	<b>1.000</b> $\pm$ 0.00	<b>1.000</b> $\pm$ 0.00	<b>1.000</b> $\pm$ 0.00	<b>1.000</b> $\pm$ 0.00	<b>1.000</b> $\pm$ 0.00	<b>0.090</b> $\pm$ 0.00	<b>0.096</b> $\pm$ 0.00
Gradient x Input	0.877 $\pm$ 0.00	0.895 $\pm$ 0.00	0.555 $\pm$ 0.01	0.210 $\pm$ 0.01	0.555 $\pm$ 0.01	0.210 $\pm$ 0.01	0.100 $\pm$ 0.00	0.086 $\pm$ 0.00
SmoothGrad	<b>1.000</b> $\pm$ 0.00	<b>1.000</b> $\pm$ 0.00	<b>1.000</b> $\pm$ 0.00	<b>1.000</b> $\pm$ 0.00	<b>1.000</b> $\pm$ 0.00	<b>1.000</b> $\pm$ 0.00	<b>0.090</b> $\pm$ 0.00	<b>0.096</b> $\pm$ 0.00
SHAP	0.854 $\pm$ 0.00	0.868 $\pm$ 0.00	0.544 $\pm$ 0.00	0.181 $\pm$ 0.01	0.544 $\pm$ 0.00	0.181 $\pm$ 0.01	0.100 $\pm$ 0.00	0.086 $\pm$ 0.00
LIME	0.950 $\pm$ 0.00	0.973 $\pm$ 0.00	0.822 $\pm$ 0.00	0.433 $\pm$ 0.01	0.822 $\pm$ 0.00	0.433 $\pm$ 0.01	<b>0.090</b> $\pm$ 0.00	<b>0.096</b> $\pm$ 0.00

**Table 17: Ground-truth and predictive faithfulness results on the German Credit dataset for all explanation methods with LR model.** Shown are average and standard error metric values computed across 1000 test instances.  $\uparrow$  indicates that higher values are better, and  $\downarrow$  indicates that lower values are better. Values corresponding to best performance are bolded.

Method	PRA ( $\uparrow$ )	RC ( $\uparrow$ )	FA ( $\uparrow$ )	RA ( $\uparrow$ )	SA ( $\uparrow$ )	SRA ( $\uparrow$ )	PGU ( $\downarrow$ )	PGI ( $\uparrow$ )
Random	0.500 $\pm$ 0.00	-0.000 $\pm$ 0.01	0.129 $\pm$ 0.01	0.014 $\pm$ 0.00	0.067 $\pm$ 0.00	0.007 $\pm$ 0.00	0.049 $\pm$ 0.00	0.011 $\pm$ 0.00
VanillaGrad	<b>1.000</b> $\pm$ 0.00	<b>1.000</b> $\pm$ 0.00	<b>1.000</b> $\pm$ 0.00	<b>1.000</b> $\pm$ 0.00	<b>1.000</b> $\pm$ 0.00	<b>1.000</b> $\pm$ 0.00	<b>0.035</b> $\pm$ 0.00	<b>0.026</b> $\pm$ 0.00
IntegratedGrad	<b>1.000</b> $\pm$ 0.00	<b>1.000</b> $\pm$ 0.00	<b>1.000</b> $\pm$ 0.00	<b>1.000</b> $\pm$ 0.00	<b>1.000</b> $\pm$ 0.00	<b>1.000</b> $\pm$ 0.00	<b>0.035</b> $\pm$ 0.00	<b>0.026</b> $\pm$ 0.00
Gradient x Input	0.465 $\pm$ 0.00	0.122 $\pm$ 0.01	0.171 $\pm$ 0.01	0.026 $\pm$ 0.00	0.171 $\pm$ 0.01	0.026 $\pm$ 0.00	0.040 $\pm$ 0.00	<b>0.026</b> $\pm$ 0.00
SmoothGrad	<b>1.000</b> $\pm$ 0.00	<b>1.000</b> $\pm$ 0.00	<b>1.000</b> $\pm$ 0.00	<b>1.000</b> $\pm$ 0.00	<b>1.000</b> $\pm$ 0.00	<b>1.000</b> $\pm$ 0.00	<b>0.035</b> $\pm$ 0.00	<b>0.026</b> $\pm$ 0.00
SHAP	0.505 $\pm$ 0.00	-0.001 $\pm$ 0.01	0.172 $\pm$ 0.01	0.025 $\pm$ 0.00	0.171 $\pm$ 0.01	0.025 $\pm$ 0.00	0.040 $\pm$ 0.00	<b>0.026</b> $\pm$ 0.00
LIME	0.977 $\pm$ 0.00	0.995 $\pm$ 0.00	0.971 $\pm$ 0.00	0.837 $\pm$ 0.01	0.971 $\pm$ 0.00	0.837 $\pm$ 0.01	<b>0.035</b> $\pm$ 0.00	<b>0.026</b> $\pm$ 0.00

**Table 18: Ground-truth and predictive faithfulness results on the COMPAS dataset for all explanation methods with LR model.** Shown are average and standard error metric values computed across 1000 test instances.  $\uparrow$  indicates that higher values are better, and  $\downarrow$  indicates that lower values are better. Values corresponding to best performance are bolded.

Method	PRA ( $\uparrow$ )	RC ( $\uparrow$ )	FA ( $\uparrow$ )	RA ( $\uparrow$ )	SA ( $\uparrow$ )	SRA ( $\uparrow$ )	PGU ( $\downarrow$ )	PGI ( $\uparrow$ )
Random	0.504 $\pm$ 0.00	0.009 $\pm$ 0.01	0.209 $\pm$ 0.01	0.137 $\pm$ 0.01	0.107 $\pm$ 0.01	0.067 $\pm$ 0.01	0.072 $\pm$ 0.00	0.029 $\pm$ 0.00
VanillaGrad	<b>1.000</b> $\pm$ 0.00	<b>1.000</b> $\pm$ 0.00	<b>1.000</b> $\pm$ 0.00	<b>1.000</b> $\pm$ 0.00	<b>1.000</b> $\pm$ 0.00	<b>1.000</b> $\pm$ 0.00	<b>0.055</b> $\pm$ 0.00	<b>0.058</b> $\pm$ 0.00
IntegratedGrad	<b>1.000</b> $\pm$ 0.00	<b>1.000</b> $\pm$ 0.00	<b>1.000</b> $\pm$ 0.00	<b>1.000</b> $\pm$ 0.00	<b>1.000</b> $\pm$ 0.00	<b>1.000</b> $\pm$ 0.00	<b>0.055</b> $\pm$ 0.00	<b>0.058</b> $\pm$ 0.00
Gradient x Input	0.622 $\pm$ 0.00	0.320 $\pm$ 0.01	0.311 $\pm$ 0.01	0.142 $\pm$ 0.01	0.311 $\pm$ 0.01	0.142 $\pm$ 0.01	0.070 $\pm$ 0.00	0.033 $\pm$ 0.00
SmoothGrad	<b>1.000</b> $\pm$ 0.00	<b>1.000</b> $\pm$ 0.00	<b>1.000</b> $\pm$ 0.00	<b>1.000</b> $\pm$ 0.00	<b>1.000</b> $\pm$ 0.00	<b>1.000</b> $\pm$ 0.00	<b>0.055</b> $\pm$ 0.00	<b>0.058</b> $\pm$ 0.00
SHAP	0.614 $\pm$ 0.00	0.287 $\pm$ 0.01	0.311 $\pm$ 0.01	0.134 $\pm$ 0.01	0.310 $\pm$ 0.01	0.134 $\pm$ 0.01	0.069 $\pm$ 0.00	0.033 $\pm$ 0.00
LIME	0.977 $\pm$ 0.00	0.981 $\pm$ 0.00	0.999 $\pm$ 0.00	0.997 $\pm$ 0.00	0.999 $\pm$ 0.00	0.997 $\pm$ 0.00	<b>0.055</b> $\pm$ 0.00	<b>0.058</b> $\pm$ 0.00

**Table 19: Ground-truth and predictive faithfulness results on the GMSC dataset for all explanation methods with LR model.** Shown are average and standard error metric values computed across 1000 test instances.  $\uparrow$  indicates that higher values are better, and  $\downarrow$  indicates that lower values are better. Values corresponding to best performance are bolded.

Method	PRA ( $\uparrow$ )	RC ( $\uparrow$ )	FA ( $\uparrow$ )	RA ( $\uparrow$ )	SA ( $\uparrow$ )	SRA ( $\uparrow$ )	PGU ( $\downarrow$ )	PGI ( $\uparrow$ )
Random	0.499 $\pm$ 0.00	-0.006 $\pm$ 0.01	0.197 $\pm$ 0.01	0.098 $\pm$ 0.01	0.098 $\pm$ 0.01	0.049 $\pm$ 0.00	0.026 $\pm$ 0.00	0.009 $\pm$ 0.00
VanillaGrad	<b>1.000</b> $\pm$ 0.00	<b>1.000</b> $\pm$ 0.00	<b>1.000</b> $\pm$ 0.00	<b>1.000</b> $\pm$ 0.00	<b>1.000</b> $\pm$ 0.00	<b>1.000</b> $\pm$ 0.00	<b>0.012</b> $\pm$ 0.00	<b>0.024</b> $\pm$ 0.00
IntegratedGrad	<b>1.000</b> $\pm$ 0.00	<b>1.000</b> $\pm$ 0.00	<b>1.000</b> $\pm$ 0.00	<b>1.000</b> $\pm$ 0.00	<b>1.000</b> $\pm$ 0.00	<b>1.000</b> $\pm$ 0.00	<b>0.012</b> $\pm$ 0.00	<b>0.024</b> $\pm$ 0.00
Gradient x Input	0.499 $\pm$ 0.00	-0.006 $\pm$ 0.01	0.124 $\pm$ 0.01	0.067 $\pm$ 0.01	0.124 $\pm$ 0.01	0.067 $\pm$ 0.01	0.023 $\pm$ 0.00	0.013 $\pm$ 0.00
SmoothGrad	<b>1.000</b> $\pm$ 0.00	<b>1.000</b> $\pm$ 0.00	<b>1.000</b> $\pm$ 0.00	<b>1.000</b> $\pm$ 0.00	<b>1.000</b> $\pm$ 0.00	<b>1.000</b> $\pm$ 0.00	<b>0.012</b> $\pm$ 0.00	<b>0.024</b> $\pm$ 0.00
SHAP	0.495 $\pm$ 0.00	-0.053 $\pm$ 0.01	0.140 $\pm$ 0.01	0.085 $\pm$ 0.01	0.140 $\pm$ 0.01	0.085 $\pm$ 0.01	0.023 $\pm$ 0.00	0.013 $\pm$ 0.00
LIME	0.909 $\pm$ 0.00	0.920 $\pm$ 0.00	0.954 $\pm$ 0.00	0.953 $\pm$ 0.00	0.954 $\pm$ 0.00	0.953 $\pm$ 0.00	<b>0.012</b> $\pm$ 0.00	<b>0.024</b> $\pm$ 0.00

**Table 20: Stability results on the HELOC dataset for all explanation methods with LR model.** Shown are log average and standard error metric values computed across 1000 test instances.  $\uparrow$  indicates that higher values are better, and  $\downarrow$  indicates that lower values are better. Values corresponding to best performance are bolded.

Method	RIS ( $\downarrow$ )	ROS ( $\downarrow$ )
Random	11.74 $\pm$ 0.00	14.10 $\pm$ 0.02
VanillaGrad	2.75 $\pm$ 0.02	1.89 $\pm$ 0.13
IntegratedGrad	<b>1.25</b> $\pm$ 0.01	<b>-0.42</b> $\pm$ 0.02
Gradient x Input	2.75 $\pm$ 0.02	3.64 $\pm$ 0.05
SmoothGrad	10.00 $\pm$ 0.03	12.27 $\pm$ 0.04
SHAP	9.68 $\pm$ 0.02	12.01 $\pm$ 0.04
LIME	9.86 $\pm$ 0.03	12.82 $\pm$ 0.04

**Table 21: Stability results on the Adult Income dataset for all explanation methods with LR model.** Shown are log average and standard error metric values computed across 1000 test instances.  $\uparrow$  indicates that higher values are better, and  $\downarrow$  indicates that lower values are better. Values corresponding to best performance are bolded.

Method	RIS ( $\downarrow$ )	ROS ( $\downarrow$ )
Random	12.95 $\pm$ 0.00	14.43 $\pm$ 0.03
VanillaGrad	3.75 $\pm$ 0.02	2.34 $\pm$ 0.06
IntegratedGrad	<b>2.61</b> $\pm$ 0.01	<b>0.23</b> $\pm$ 0.02
Gradient x Input	3.79 $\pm$ 0.02	3.46 $\pm$ 0.04
SmoothGrad	11.41 $\pm$ 0.04	13.33 $\pm$ 0.11
SHAP	11.36 $\pm$ 0.02	12.12 $\pm$ 0.03
LIME	11.35 $\pm$ 0.04	14.23 $\pm$ 0.04

**Table 22: Stability results on the COMPAS dataset for all explanation methods with LR model.** Shown are log average and standard error metric values computed across 1000 test instances.  $\uparrow$  indicates that higher values are better, and  $\downarrow$  indicates that lower values are better. Values corresponding to best performance are bolded.

Method	RIS ( $\downarrow$ )	ROS ( $\downarrow$ )
Random	13.11 $\pm$ 0.01	14.04 $\pm$ 0.02
VanillaGrad	2.33 $\pm$ 0.02	1.86 $\pm$ 0.15
IntegratedGrad	<b>1.49</b> $\pm$ 0.01	<b>0.06</b> $\pm$ 0.02
Gradient x Input	2.41 $\pm$ 0.01	4.37 $\pm$ 0.05
SmoothGrad	11.39 $\pm$ 0.02	13.72 $\pm$ 0.04
SHAP	10.02 $\pm$ 0.02	12.00 $\pm$ 0.03
LIME	10.64 $\pm$ 0.02	11.87 $\pm$ 0.04

**Table 23: Stability results on the GMSC dataset for all explanation methods with LR model.** Shown are log average and standard error metric values computed across 1000 test instances.  $\uparrow$  indicates that higher values are better, and  $\downarrow$  indicates that lower values are better. Values corresponding to best performance are bolded.

Method	RIS ( $\downarrow$ )	ROS ( $\downarrow$ )
Random	11.47 $\pm$ 0.01	14.97 $\pm$ 0.01
VanillaGrad	2.77 $\pm$ 0.02	2.86 $\pm$ 0.04
IntegratedGrad	<b>1.87</b> $\pm$ 0.01	<b>1.27</b> $\pm$ 0.02
Gradient x Input	2.84 $\pm$ 0.02	4.79 $\pm$ 0.04
SmoothGrad	10.52 $\pm$ 0.03	11.97 $\pm$ 0.01
SHAP	9.25 $\pm$ 0.02	13.18 $\pm$ 0.02
LIME	10.44 $\pm$ 0.04	13.48 $\pm$ 0.04

## D.7 Remaining Results on ANN models

**Table 24: Predictive faithfulness results on the Synthetic dataset for all explanation methods with ANN model.** Shown are average and standard error metric values computed across 1000 test instances.  $\uparrow$  indicates that higher values are better, and  $\downarrow$  indicates that lower values are better. Values corresponding to best performance are bolded.

Method	PGU ( $\downarrow$ )	PGI ( $\uparrow$ )
Random	0.143 $\pm$ 0.005	0.053 $\pm$ 0.003
VanillaGrad	0.107 $\pm$ 0.004	0.116 $\pm$ 0.004
IntegratedGrad	0.116 $\pm$ 0.004	0.102 $\pm$ 0.004
Gradient x Input	0.113 $\pm$ 0.004	0.109 $\pm$ 0.004
SmoothGrad	0.106 $\pm$ 0.004	0.116 $\pm$ 0.004
SHAP	0.124 $\pm$ 0.005	0.092 $\pm$ 0.004
LIME	<b>0.105</b> $\pm$ 0.004	<b>0.117</b> $\pm$ 0.004

**Table 25: Predictive faithfulness results on the German Credit dataset for all explanation methods with ANN model.** Shown are average and standard error metric values computed across 1000 test instances.  $\uparrow$  indicates that higher values are better, and  $\downarrow$  indicates that lower values are better. Values corresponding to best performance are bolded.

Method	PGU ( $\downarrow$ )	PGI ( $\uparrow$ )
Random	0.120 $\pm$ 0.007	0.030 $\pm$ 0.002
VanillaGrad	0.104 $\pm$ 0.007	0.056 $\pm$ 0.004
IntegratedGrad	0.105 $\pm$ 0.007	0.053 $\pm$ 0.004
Gradient x Input	<b>0.103</b> $\pm$ 0.007	<b>0.065</b> $\pm$ 0.004
SmoothGrad	<b>0.103</b> $\pm$ 0.007	0.057 $\pm$ 0.004
SHAP	<b>0.103</b> $\pm$ 0.007	0.063 $\pm$ 0.004
LIME	0.104 $\pm$ 0.007	0.056 $\pm$ 0.004

**Table 26: Predictive faithfulness results on the HELOC dataset for all explanation methods with ANN model.** Shown are average and standard error metric values computed across 1000 test instances.  $\uparrow$  indicates that higher values are better, and  $\downarrow$  indicates that lower values are better. Values corresponding to best performance are bolded.

Method	PGU ( $\downarrow$ )	PGI ( $\uparrow$ )
Random	0.107 $\pm$ 0.003	0.042 $\pm$ 0.002
VanillaGrad	<b>0.082</b> $\pm$ 0.003	0.081 $\pm$ 0.003
IntegratedGrad	0.084 $\pm$ 0.003	0.079 $\pm$ 0.003
Gradient x Input	0.106 $\pm$ 0.003	0.046 $\pm$ 0.002
SmoothGrad	<b>0.082</b> $\pm$ 0.003	<b>0.082</b> $\pm$ 0.003
SHAP	0.106 $\pm$ 0.003	0.044 $\pm$ 0.002
LIME	<b>0.082</b> $\pm$ 0.003	0.081 $\pm$ 0.003

**Table 27: Predictive faithfulness results on the Adult Income dataset for all explanation methods with ANN model.** Shown are average and standard error metric values computed across 1000 test instances.  $\uparrow$  indicates that higher values are better, and  $\downarrow$  indicates that lower values are better. Values corresponding to best performance are bolded.

Method	PGU ( $\downarrow$ )	PGI ( $\uparrow$ )
Random	0.207 $\pm$ 0.004	0.069 $\pm$ 0.003
VanillaGrad	0.071 $\pm$ 0.003	0.230 $\pm$ 0.004
IntegratedGrad	<b>0.070</b> $\pm$ 0.003	<b>0.233</b> $\pm$ 0.004
Gradient x Input	0.221 $\pm$ 0.004	0.071 $\pm$ 0.003
SmoothGrad	<b>0.070</b> $\pm$ 0.003	0.230 $\pm$ 0.004
SHAP	0.223 $\pm$ 0.004	0.068 $\pm$ 0.003
LIME	0.071 $\pm$ 0.003	0.230 $\pm$ 0.004

**Table 28: Predictive faithfulness results on the COMPAS dataset for all explanation methods with ANN model.** Shown are average and standard error metric values computed across 1000 test instances.  $\uparrow$  indicates that higher values are better, and  $\downarrow$  indicates that lower values are better. Values corresponding to best performance are bolded.

Method	PGU ( $\downarrow$ )	PGI ( $\uparrow$ )
Random	0.095 $\pm$ 0.004	0.035 $\pm$ 0.002
VanillaGrad	<b>0.056</b> $\pm$ 0.003	<b>0.090</b> $\pm$ 0.004
IntegratedGrad	<b>0.056</b> $\pm$ 0.003	<b>0.090</b> $\pm$ 0.004
Gradient x Input	0.073 $\pm$ 0.003	0.068 $\pm$ 0.003
SmoothGrad	<b>0.056</b> $\pm$ 0.003	<b>0.090</b> $\pm$ 0.004
SHAP	0.073 $\pm$ 0.003	0.072 $\pm$ 0.003
LIME	0.057 $\pm$ 0.003	<b>0.090</b> $\pm$ 0.004

**Table 29: Predictive faithfulness results on the GMSC dataset for all explanation methods with ANN model.** Shown are average and standard error metric values computed across 1000 test instances.  $\uparrow$  indicates that higher values are better, and  $\downarrow$  indicates that lower values are better. Values corresponding to best performance are bolded.

Method	PGU ( $\downarrow$ )	PGI ( $\uparrow$ )
Random	0.088 $\pm$ 0.003	0.026 $\pm$ 0.002
VanillaGrad	<b>0.015</b> $\pm$ 0.001	<b>0.102</b> $\pm$ 0.003
IntegratedGrad	<b>0.015</b> $\pm$ 0.001	<b>0.102</b> $\pm$ 0.003
Gradient x Input	0.059 $\pm$ 0.002	0.063 $\pm$ 0.003
SmoothGrad	<b>0.015</b> $\pm$ 0.001	<b>0.102</b> $\pm$ 0.003
SHAP	0.067 $\pm$ 0.002	0.053 $\pm$ 0.003
LIME	<b>0.015</b> $\pm$ 0.001	0.101 $\pm$ 0.003



**Table 30: Stability results on the Synthetic dataset for all explanation methods with ANN model.** Shown are log average and standard error metric values computed across 1000 test instances.  $\uparrow$  indicates that higher values are better, and  $\downarrow$  indicates that lower values are better. Values corresponding to best performance are bolded.

Method	RIS ( $\downarrow$ )	RRS ( $\downarrow$ )	ROS ( $\downarrow$ )
Random	11.58 $\pm$ 0.00	10.80 $\pm$ 0.01	15.12 $\pm$ 0.04
VanillaGrad	5.29 $\pm$ 0.20	4.23 $\pm$ 0.22	5.47 $\pm$ 0.48
IntegratedGrad	<b>3.56</b> $\pm$ 0.17	<b>2.51</b> $\pm$ 0.20	5.79 $\pm$ 0.39
Gradient x Input	5.21 $\pm$ 0.18	4.13 $\pm$ 0.20	<b>5.33</b> $\pm$ 0.37
SmoothGrad	31.27 $\pm$ 1.00	30.62 $\pm$ 1.00	32.06 $\pm$ 1.00
SHAP	10.55 $\pm$ 0.02	9.74 $\pm$ 0.02	13.94 $\pm$ 0.04
LIME	21.11 $\pm$ 0.89	20.60 $\pm$ 0.91	21.70 $\pm$ 0.82

**Table 31: Stability results on the German Credit dataset for all explanation methods with ANN model.** Shown are log average and standard error metric values computed across 1000 test instances.  $\uparrow$  indicates that higher values are better, and  $\downarrow$  indicates that lower values are better. Values corresponding to best performance are bolded.

Method	RIS ( $\downarrow$ )	RRS ( $\downarrow$ )	ROS ( $\downarrow$ )
Random	12.84 $\pm$ 0.00	12.77 $\pm$ 0.01	16.06 $\pm$ 0.06
VanillaGrad	3.18 $\pm$ 0.31	3.06 $\pm$ 0.36	<b>3.24</b> $\pm$ 0.43
IntegratedGrad	<b>2.16</b> $\pm$ 0.33	<b>1.98</b> $\pm$ 0.34	4.34 $\pm$ 0.36
Gradient x Input	3.19 $\pm$ 0.31	3.06 $\pm$ 0.36	3.96 $\pm$ 0.21
SmoothGrad	11.57 $\pm$ 0.06	11.47 $\pm$ 0.06	14.40 $\pm$ 0.11
SHAP	11.80 $\pm$ 0.01	11.77 $\pm$ 0.02	15.13 $\pm$ 0.07
LIME	11.77 $\pm$ 0.05	11.73 $\pm$ 0.05	14.78 $\pm$ 0.10

**Table 32: Stability results on the HELOC dataset for all explanation methods with ANN model.** Shown are log average and standard error metric values computed across 1000 test instances.  $\uparrow$  indicates that higher values are better, and  $\downarrow$  indicates that lower values are better. Values corresponding to best performance are bolded.

Method	RIS ( $\downarrow$ )	RRS ( $\downarrow$ )	ROS ( $\downarrow$ )
Random	11.74 $\pm$ 0.00	11.52 $\pm$ 0.01	15.16 $\pm$ 0.04
VanillaGrad	3.53 $\pm$ 0.17	3.00 $\pm$ 0.23	4.49 $\pm$ 0.50
IntegratedGrad	<b>2.47</b> $\pm$ 0.07	<b>2.03</b> $\pm$ 0.09	<b>4.10</b> $\pm$ 0.18
Gradient x Input	3.69 $\pm$ 0.23	3.18 $\pm$ 0.29	5.32 $\pm$ 0.33
SmoothGrad	10.96 $\pm$ 0.08	10.85 $\pm$ 0.07	13.91 $\pm$ 0.06
SHAP	10.69 $\pm$ 0.02	10.54 $\pm$ 0.02	14.32 $\pm$ 0.04
LIME	10.42 $\pm$ 0.05	10.32 $\pm$ 0.05	14.02 $\pm$ 0.08

**Table 33: Stability results on the Adult Income dataset for all explanation methods with ANN model.** Shown are log average and standard error metric values computed across 1000 test instances.  $\uparrow$  indicates that higher values are better, and  $\downarrow$  indicates that lower values are better. Values corresponding to best performance are bolded.

Method	RIS ( $\downarrow$ )	RRS ( $\downarrow$ )	ROS ( $\downarrow$ )
Random	12.95 $\pm$ 0.00	12.03 $\pm$ 0.01	14.75 $\pm$ 0.05
VanillaGrad	5.73 $\pm$ 0.07	3.98 $\pm$ 0.16	3.58 $\pm$ 0.33
IntegratedGrad	<b>3.81</b> $\pm$ 0.11	<b>1.97</b> $\pm$ 0.13	<b>3.38</b> $\pm$ 0.07
Gradient x Input	5.79 $\pm$ 0.10	4.02 $\pm$ 0.15	4.20 $\pm$ 0.17
SmoothGrad	13.33 $\pm$ 0.31	13.98 $\pm$ 0.39	17.08 $\pm$ 0.45
SHAP	13.31 $\pm$ 0.09	12.01 $\pm$ 0.09	14.49 $\pm$ 0.12
LIME	10.83 $\pm$ 0.01	9.67 $\pm$ 0.02	12.95 $\pm$ 0.06

**Table 34: Stability results on the COMPAS dataset for all explanation methods with ANN model.** Shown are log average and standard error metric values computed across 1000 test instances.  $\uparrow$  indicates that higher values are better, and  $\downarrow$  indicates that lower values are better. Values corresponding to best performance are bolded.

Method	RIS ( $\downarrow$ )	RRS ( $\downarrow$ )	ROS ( $\downarrow$ )
Random	13.11 $\pm$ 0.01	12.88 $\pm$ 0.01	15.30 $\pm$ 0.03
VanillaGrad	4.68 $\pm$ 0.18	3.96 $\pm$ 0.19	4.30 $\pm$ 0.53
IntegratedGrad	<b>3.59</b> $\pm$ 0.04	<b>2.83</b> $\pm$ 0.05	<b>3.86</b> $\pm$ 0.30
Gradient x Input	4.99 $\pm$ 0.30	4.30 $\pm$ 0.32	5.46 $\pm$ 0.42
SmoothGrad	17.33 $\pm$ 0.13	17.21 $\pm$ 0.12	18.09 $\pm$ 0.10
SHAP	10.55 $\pm$ 0.02	10.39 $\pm$ 0.01	12.80 $\pm$ 0.04
LIME	15.23 $\pm$ 0.10	15.13 $\pm$ 0.09	16.37 $\pm$ 0.11

**Table 35: Stability results on the GMSC dataset for all explanation methods with ANN model.** Shown are log average and standard error metric values computed across 1000 test instances.  $\uparrow$  indicates that higher values are better, and  $\downarrow$  indicates that lower values are better. Values corresponding to best performance are bolded.

Method	RIS ( $\downarrow$ )	RRS ( $\downarrow$ )	ROS ( $\downarrow$ )
Random	11.47 $\pm$ 0.01	11.51 $\pm$ 0.01	14.72 $\pm$ 0.04
VanillaGrad	4.44 $\pm$ 0.09	3.78 $\pm$ 0.11	<b>4.22</b> $\pm$ 0.55
IntegratedGrad	<b>3.63</b> $\pm$ 0.02	<b>2.94</b> $\pm$ 0.03	4.40 $\pm$ 0.26
Gradient x Input	4.59 $\pm$ 0.11	3.96 $\pm$ 0.14	5.57 $\pm$ 0.48
SmoothGrad	10.35 $\pm$ 0.03	10.28 $\pm$ 0.03	13.29 $\pm$ 0.05
SHAP	9.94 $\pm$ 0.02	9.94 $\pm$ 0.01	12.73 $\pm$ 0.06
LIME	9.77 $\pm$ 0.03	9.76 $\pm$ 0.03	13.65 $\pm$ 0.05

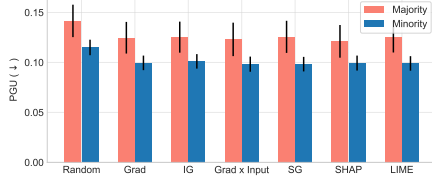


**Figure 3: Fairness analysis of PGU metric on the German Credit dataset with ANN model.** Shown are average and standard error values for majority (male) and minority (female) subgroups. Larger gaps between the values of majority and minority subgroups (i.e. red and blue bars respectively) indicate higher disparities which are undesirable.

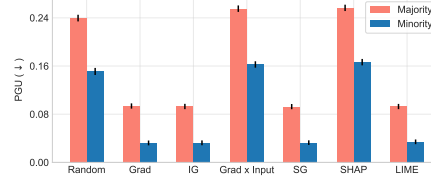


**Figure 4: Fairness analysis of PGU metric on the Adult Income dataset with ANN model.** Shown are average and standard error values for majority (male) and minority (female) subgroups. Larger gaps between the values of majority and minority subgroups (i.e. red and blue bars respectively) indicate higher disparities which are undesirable.

## E Choice of XAI methods, datasets, and models

While feature attribution-based explanation methods such as LIME, SHAP, and Gradient-based methods have been proposed a few years back, they continue to be the most popular and widely used post hoc explanation methods both in research [16, 43, 7, 33, 31] and in practice [23, 78, 34, 28]. In fact, several recent works published in 2022 have analyzed these methods both theoretically and empirically, and have called for further study of these methods given their widespread adoption [19, 16, 9, 31, 43, 26]. Furthermore, recent research has also argued that there is little to no understanding of the behavior and effectiveness of even basic post hoc explanation methods such as LIME, SHAP, and gradient-based methods [43, 50, 64, 40, 10, 3], and developing such an understanding would be a critical first step towards the progress of the XAI field. To this end, we focus on these methods for the first release of our OpenXAI framework. In the next release, we plan to evaluate and benchmark other recently proposed methods (e.g., TCAV and its extensions, influence functions, etc.) as well.

Note that the evaluation metrics and the explanation methods that we include in our framework are generic enough to be applicable to other modalities of data including text and images. The reason why we focused on tabular data for the first release of OpenXAI is two-fold: i) The need for model understanding and explainability is often motivated by high-stakes decision-making settings and applications e.g., loan approvals, disease diagnosis and treatment recommendations, recidivism prediction etc. [14, 57, 58]. Data encountered in these settings is predominantly tabular. ii) Recent research has argued that there is no clear understanding as to which explanation methods perform well on what kinds of metrics even on simple, low-dimensional tabular datasets [50, 19, 43, 31], and that this is a big open question which has far reaching implications for the progress of the field. To this end, we focused on tabular data for the first release of OpenXAI so that we could find some answers to the aforementioned question in the context of simple, low-dimensional tabular datasets before proceeding to high-dimensional image and text datasets. In the next release of OpenXAI, we plan to include and support image and text datasets, and also add metrics and explanation methods that are specific to these new data modalities.

The datasets that we utilize in this work are very popular and are widely employed in XAI and fairness research till date. For instance, several recent works in XAI published at ICML, NeurIPS, and FAccT conferences in 2021-22 have employed these datasets both to evaluate the efficacy of newly proposed methods, as well as to study the behavior of existing methods [9, 18–20, 38, 69, 73, 5]. Given this, we follow suit and employ these datasets in our benchmarking efforts. Similarly, the aforementioned works also employ logistic regression models and deep neural network architectures similar to the ones considered in our research.